Chapter 2
Sub-Nucleonic Structure and the Modern Picture of Isotopes

2.1 History and Overview

Investigations of the *atomic nucleus*, and the fundamental forces that determine *nuclear* structure as is well known offer fascinating insights into the nature of the physical world [1–10]. We all known well that the history of the nuclear physics dates from the latter years of the nineteenth century when Henry Becqeurel in 1896 discovered the radioactivity. He was working with compounds containing the element uranium. Becqeurel found that photographic plates covered to keep out light became fogged, or partially exposed, when these uranium compounds were anywhere near the plates. Two years after Becquerel's discovery, Pierre and Marie Curie in France and Rutherford in England succeeded in separating a naturally occurring radioactive element, radium ($Z = 88$), from the ore. It was soon revealed that there are three, distinctly different types of radiation emitted by radioactive substances. They were called *alpha* (α), *beta* (β) and *gamma* (γ) rays—terms which have been retained in ours days. When a radioactive source was placed in a magnetic field, it was found that there were three different activities, as the trajectories of some of the rays emitted were deflected to one direction, some to the opposite direction and some not affected at all. Subsequently it was found that α-rays consist of positively charged ^{4}He nuclei, β-rays are made of electrons (positrons) and γ-rays are nothing but electromagnetic radiation that carries no net charge. The existence of the nucleus as the small central part of an atom was first proposed by Rutherford in 1911. Rutherford proposed that the atom does consist of a small, heavy positively charged centre surrounded by orbiting electrons which occupy the vast bulk of the atoms volume. The simplest atom—hydrogen—consisted of a proton and a single orbital electron. Later, in 1920, the radii of a few heavy nuclei were measured by Chadwick and were found to be in the order of 10^{-14} m, much smaller than the order of 10^{-10} m for atomic radii (for details, see e.g. [4–9]).

The building blocks of nuclei are *neutrons* and *protons*, two aspects, or quantum states, of the same particle, the *nucleon*. Since a neutron does not carry any net electric charge and is unstable as an isolated particle (see, below), it was not discovered

V. G. Plekhanov, *Isotopes in Condensed Matter*, Springer Series in Materials Science 162,
DOI: 10.1007/978-3-642-28723-7_2, © Springer-Verlag Berlin Heidelberg 2013

Table 2.1 Fundamental interactions

Interaction	FQ	Mass	Range (m)	RS	Spin	T C-S (m^2)	TTS (s)
Strong	Gluon	0	10^{-15}	1	1	10^{-30}	10^{-23}
Weak	$W^{\mp}$; Z	81; 93 GeV/c^2	10^{-18}	10^{-5}	1;1	10^{-44}	10^{-8}
Electromagnetic	Photon	0	∞	$\alpha = 1/137$	1	10^{-33}	10^{-20}
Gravity	Graviton	0	∞	10^{-30}	2	–	–

Here *FQ* field quant, *RS* relative strength, *TC-S* typical cross-section, *TTS* typical time scale

until 1932 by Chadwick, whose existence has been anticipated by Rutherford as early as 1920. Since only positive charges (protons) are present in nucleus, the electromagnetic force inside a nucleus is repulsive and the nucleons cannot be held together unless there is another source of force that is attractive and stronger than Coulomb's (see, also [10]). Here we have our first encounter with *strong interaction* (see, also Table 2.1). In 1934 Hideki Yukawa proposed the first significant theory of the *strong force* to explain how the nucleus holds together. As we know, with Fermi and Yukawa's papers the modern model of the atom was complete [2–6].

Studies of the structure of the nucleus have shown that it is composed of protons and neutrons, and more recently studies [11–14] of very high energy collisions have shown that these protons and neutrons are themselves composed of elusive particles called *quarks*. Particle physics deals with the world of the quarks and all other particles still thought to be fundamental. One may argue that, since nuclear force is only one aspect of the strong interaction between quarks, all we need therefore to do is to understand *quantum chromodynamics* (QCD)[1] (for details see [12–15] and below). The structure of neutrons and protons is discerned only at very high energies (see, e.g. [15]) and, for all practical purpose concerning nuclear structure, research and nuclear physics applications in the modern world, the neutron–proton model of the nucleus is entirely adequate.

Thus, our present knowledge of physical phenomena suggests that there are four types of forces between physical objects:

1. Gravitational;
2. Electromagnetic;
3. Strong and
4. Weak.

Both *gravitational* and *electromagnetic* forces are infinite in range and their interaction strength diminishes with the square of the distance of separation. Clearly, nuclear force cannot follow the same radial dependence. Being much stronger, it would have pulled the nucleons in different nuclei together into a single unit and destroy all the atomic structure we are familiar with. In fact, *nuclear force* has a

[1] QCD is the modern theory of the strong interaction. QCD, the theory of quarks, gluons and their interactions, is a self-contained part of the Standard Model (see below) of elementary particles. Historically its route is in nuclear physics and the description of ordinary matter—understanding what protons and neutrons are (and their structure) and how they interact. Nowadays QCD is used to describe most of what goes at high-energy accelerators.

very short distance. As we know at present time, only three particles, the proton, the electron and the photon, are stable. Another particle, the neutron, is stable when it is bound within a nucleus, and is unstable with life time of 887 ± 2 s when it is free (for details see, also [11–14]). Since nuclei are involved in a wide variety of applied and pure research, nuclear physics overlaps with a number of other fields of physics: particles; astrophysics; stellar evolution, etc. Therefore, the primary aim of nuclear physics is to understand the force between nucleons, the structure of nuclei and how nuclei interact with each other and with other *subatomic particles*. These three questions are, to a large extent, related with each other. Much of the current research in nuclear physics (see, e.g. [1–10]) relates to the study of nuclei under extreme conditions such as high spin and excitation energy. Nuclei may also have extreme shapes (for instance similar to that American footballs) or extreme neutron-to-proton ratios. Modern experimenters can create such nuclei using artificially induced fusion or nucleon transfer reactions, employing ion beams from different sources. Beams with even higher energies (e.g. from accelerator) can be used to create nuclei at very high temperatures, and there are signs that these experiments have produced phase transition from normal nuclear matter to a new state, the quarks condensate, the quark-gluon plasma, in which the quarks mingle with one another, rather than being segregated in triplets as they are in neutrons and protons.

If in the nuclear physics the meaning of isotope is establishing one [7, 9, 10, 15], then application of isotope effect in atomic [16–19] and molecular [20–22] physics allows to get the results, which are difficult to overestimate so far as owing to this results it was to construct the "building" of the science of the twentieth century—the quantum mechanics. In the last 50 years the isotope effect is one of the modern and power methods used in investigation of structure and properties of solids. This conclusion supports the numerous reviews (see, e.g. [23–25]) and first monographs [26, 27, 29] dedicated to isotope effect of stable isotopes. In the last years, more and more investigations of solid-state physics are conducted by using *radioactive isotopes*, which give evidence of already comprehensive list of references (see, for instance [28, 30, 31]). It is a well known fact that large and successful application of the radioactive elements in medicine [32–35], the direction in isotope physics, is more finance supportive in different states (see, for example, [36] and references therein). Moreover, it is obviously a leading role of the isotope physics in the study of the nature–nuclear interactions and reconstruction of nucleogenesys process in the Universe [37–40] which could be explained as the observable in nature relative to spreading of chemical elements.

Such wide field of isotope applications stimulate necessity for examination and critical analysis from point of view of the microscopical nature of isotope effect.[2]

[2] With the aim of the ground of nature of isotope effect, a detailed analysis of the neutron and proton structure and their mutual transformation in the *weak interaction* process was conducted. Note that the main characteristics of isotope effect—the mass of free particles (proton and neutron)—does not conserve in the weak interaction process. This contradiction is removed although partly if we take into account the modern presentation [42–44] that the mass of proton (neutron) is created from quark condensate (not from constituent quarks [15, 44]) which is the coherent superposition of the states with different chirality. Thus the elucidation of the reason of origin of the nucleon

Table 2.2 The basic properties of the atomic constituents

Particle	Charge	Mass (u)	Spin ($\hbar$)	Magnetic moment (JT^{-1})
Proton	e	1.007276	1/2	1.411×10^{-26}
Neutron	0	1.008665	1/2	-9.66×10^{-27}
Electron	$-$e	0.000549	1/2	9.28×10^{-24}

Such approach to isotope physics allows to make known not only the intrinsic contradiction inherent this area of physics but also determine the borders of the effect. A step-by-step comparison with existing theoretical models not only reveals the degree of agreement (or disagreement) but also provides a new impulse for both the development of new theoretical ideas and for conducting new experiments (see, also [41]).

2.2 The Structure of Atomic Nucleus

An atom consists of an extremely small, positively charged nucleus (see Fig. 2.1) surrounded by a cloud of negatively charged electrons. Although typically the nucleus is less than one ten-thousandth the size of the atom, the nucleus contains more than 99.9% of the mass of the atom. Atomic nucleus is the small, central part of an atom consisting of A-nucleons, Z-protons and N-neutrons (Fig. 2.2). The atomic mass of the nucleus, A, is equal to Z+N. A given element can have many different isotopes, which differ from one another by the number of neutrons contained in the nuclei [58, 59]. In a neutral atom, the number of electrons orbiting the nucleus equals the number of protons in the nucleus. As usual, *nuclear size* is measured in fermis ($1\text{fm} = 10^{-15}$ m, also called femtometers). The basic properties of the atomic constituents can be read in Table 2.2.

As we can see from this table, protons have a positive charge of magnitude $e = 1.6022 \times 10^{-19}$ C (Coulomb's) equal and opposite to that of the electrons. Neutrons are uncharged. Thus a neutral atom (A, Z) contains Z electrons and can be written symbolically as ${}^{A}_{Z}X_{N}$ (see also Fig. 2.2). Here X is chemical symbol and N is neutron number and is equal $N = A - Z$.[3] The masses of proton and neutron are almost the same, approximately 1836 and 1839 electron masses (m_e), respectively. Apart from electric charge, the proton and neutron have almost the same properties. This is why there is a common name of them: *nucleon*. Both the proton and neutron are nucleons.

(Footnote 2 continued)
mass is taken down to elucidation of the reason to break down the chiral symmetry in *Quantum Chromodynamics* [45–56].

[3] Nuclei with the same N and different Z are called *isotones*, and *nuclides* with the same mass number A are known as *isobars*. In a symbolic representation of a nuclear specie or nuclide, it is usual to omit the N and Z subscripts and include only the mass number as a superscript, since A = N+Z and the symbol X represents the chemical elements.

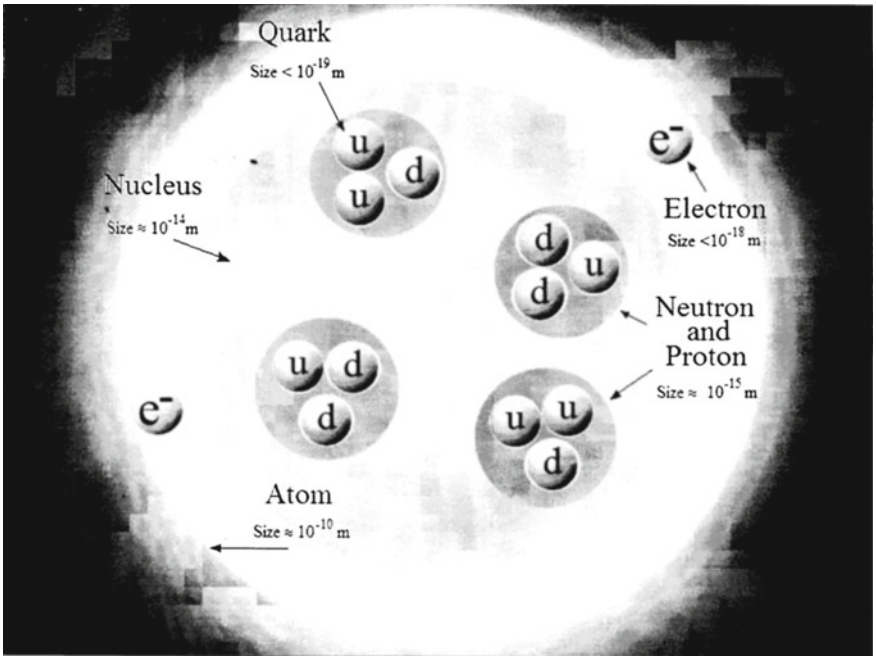

Fig. 2.1 Structure within the atom. If the protons and neutrons in this picture were 10 cm across, then the quarks and electrons would be less than 0.1 mm in size and the entire atom would be about 10 km across (after http://www.lbl.gov/abc/wallchart/)

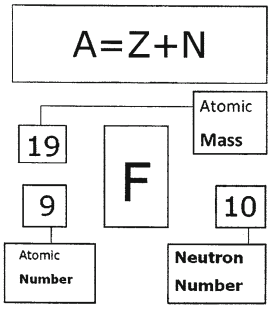

Fig. 2.2 Atomic nomenclature

We know well that the proton is denoted by letter p and the neutron by n. Chemical properties of an element are determined by the charge of its atomic nucleus, i.e. by the number of protons (electrons). It should be added that although it is true that the neutron has zero net charge, it is nonetheless composed of electrically charged quarks (see below), in the same way that a neutral atom is nonetheless composed of protons and electrons. As such, the neutron experiences the electromagnetic interaction. The net charge is zero, so if we are far enough away from the neutron that it appears to occupy no volume, then the total effect of the electric force will add up to zero. The

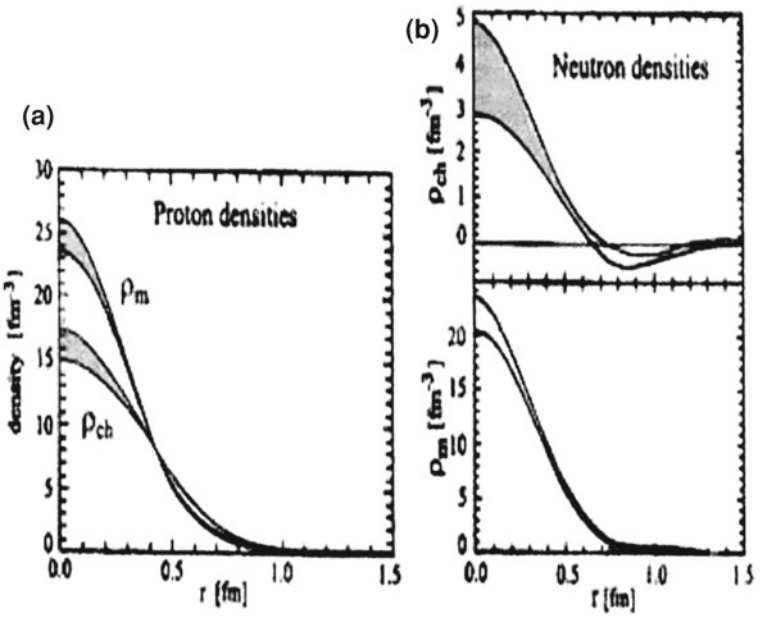

Fig. 2.3 Comparison between charge (ρ_{ch}) and magnetization (ρ_m) for the proton (**a**) and neutron (**b**). Both densities are normalized to $\int \mathrm{drr}^2\rho = 1(\mathrm{r})$ (after [62–64])

movement of the charges inside the neutrons does not cancel, however, and this is what gives the neutron its non-zero magnetic moment.

Each of the atomic constituencies, a spin 1/2 in units of $\hbar(=h/2\pi)$ and is an example of the class of particles of half-integer spin known as fermions. Fermions obey the exclusion principle of Pauli (see, e.g. [9]), which determines the way electrons can occupy atomic energy states. The same rule applies, as will be shown below, to nucleons in nuclei. Associated with the spin is a magnetic dipole moment. Compared with the magnetic moment of electron, nuclear moment is very small. However, they play an important role in the theory of nuclear structure. It may be surprising that the uncharged neutron has a magnetic moment. This reflects the fact that it has an underlying *quark substructure* (see, e.g. [60]), consisting of charged components. Electron scattering off these basic nuclear constituents (proton and neutron) makes up for the ideal probe to obtain a detailed view of the internal structure. A very detailed analysis using the best available data has been carried out recently by Kelly [61]. These data originate from recoil or target polarizations experiments (see, also [62–64]). In Fig. 2.3, the proton charge and magnetization distribution are given. What should be noted is the softer charge distribution compared to the magnetic one for proton. These resulting densities are quite similar to Gaussian density distributions that can be expected starting from quark picture (for details, see below) and, at the same time more realistic than the exponential density distributions [61]. The neutron charge and magnetization are also given in Fig. 2.3. What is striking is that

Table 2.3 Sample values of nuclear magnetic dipole moments (after [65])

Nuclide	$\mu(\mu_N)$
n	− 1.9130418
p	+ 2.7928456
^{2}H(D)	+ 0.8574376
^{17}O	− 1.89379
^{57}Fe	+ 0.09062293
^{57}Co	+ 4.733
^{93}Nb	+ 6.1705

magnetization distribution resembles very closely the corresponding proton distribution. Since scattering on neutrons normally carries the larger error (see, e.g. [6, 7]), the neutron charge distribution is not precisely fixed. Nonetheless, one notices that the interior charge density is balanced by a negative charge density, situated at the neutron surface region, thereby making up for the integral vanishing of the total charge of the neutron.

We may recall from atomic physics that the quantity e$\hbar$/2m is called *magneton*. For atomic motion we use the electron mass and obtain the Bohr magneton $\mu_{\mathrm{B}} = 5.7884\times10^{-5}$ eV/T. Putting in the proton mass we have the nuclear magneton $\mu_{\mathrm{N}} = 3.1525\times10^{-8}$ eV/T. Note that $\mu_N \ll \mu_B$ owing to the difference in the masses, thus, under most circumstances atomic magnetism has much larger effects than *nuclear* magnetism. Ordinary magnetic interactions of matter (ferromagnetism, for example) are determined by *atomic magnetism*.

We can write

$$\mu = \mathrm{g}_l l \mu_N, \tag{2.1}$$

where g_l is the *g-factor* associated with the orbital angular momentum l. For protons $g_l = 1$, because neutrons have no electric charge; we can use Eq. (2.1) to describe the orbital motion of neutrons if we put $g_l = 0$. We have thus been considering only the orbital motion of nucleons. Protons and neutrons, like electrons, as above mentioned above also have intrinsic or spin magnetic moments, which have no classical analog but which we write in the same form as Eq (2.1):

$$\mu = g_s s \mu_N, \tag{2.2}$$

where $s = 1/2$ for protons, neutrons and electrons (see Table 2.2). The quantity g_s is known as the spin *g-factor* and is calculated by solving a relativistic quantum mechanics equation (see, also [9]). For free nucleons, the experimental values are far from the expected value for point particles: proton—$g_s = 5.5856912 \pm 0.0000022$ and neutron—$g_s = 3.8260837 \pm 0.0000018$. Table 2.3 gives some representative values of nuclear magnetic dipole moments according [65]. The next non-vanishing moment is the electric quadrupole moment. The *quadrupole moment* eQ of a classical point charge e is of the form $e(3z^2 - r^2)$. If the particle moves with spherical symmetry, then (on the average) $z^2 = x^2 = y^2 = r^2/3$ and the

Table 2.4 Some values of nuclear electric quadrupole moments (after [65])

^{2}H(D)	+ 0.00288
^{17}O	− 0.02578
^{59}Co	+ 0.40
^{63}Cu	− 0.209
^{133}Cs	− 0.003
^{161}Dy	+ 2.4
^{176}Lu	+ 8.0
^{209}Bi	− 0.37

quadrupole moment vanishes (for details, see [8]). Some examples of the values of *nuclear electric quadrupole moments* are presented in Table 2.4.

Inside a nucleus, neutrons and protons interact with each other and are bound within (as mentioned above) the nuclear volume under the competing influences of attractive nuclear and repulsive electromagnetic forces. This binding energy has a direct effect on the mass of an atom. It is therefore not possible to separate a discussion of nuclear binding energy; if it were, then nucleon would have masses given by $Z_{m_p} + Z_{m_n}$ and the subject would hardly be of interest.

As it is well known, in 1905, Einstein presented the equivalence relationship between mass and energy: $E = mc^2$. From this formula, we see that the speed of light c is very large and so even a small mass is equivalent to a large amount of energy. This is why in nuclear physics it is more convenient to use a much smaller unit called *mega electron volt* ($1\ \text{MeV} = 1.602 \times 10^{-13}$ J). On the atomic scale, 1u is equivalent to 931.5 MeV/c^2, which is why energy changes in atoms of a few electron-volt cause insignificant changes in the mass of atom. Nuclear energies, on the other hand, are millions of electron-volts and their effects on atomic mass are easily detectable. For example, the theoretical mass of $^{35}_{17}$Cl is $17 \times 1.00782503 + 18 \times\ 1.00866491 = 35.28899389$ amu. Its measured (see below) mass is only 34.96995 amu. Therefore, the mass defect and binding energy of $^{35}_{17}$Cl are

$$\begin{aligned} \Delta &= 0.32014389\ \text{amu.} \\ E_B &= \frac{0.32014389 \times 931.5}{35} = 8.520\ \text{MeV/nucleon} \end{aligned} \tag{2.3}$$

and in common sense the binding energy is determined by next relation

$$E_B = Zm_p + Nm_n - B/c^2, \tag{2.4}$$

where B/c^2 is the actual nuclear mass.

As we can see below, the *binding energy* of the atoms of most elements have values ranging from about 7.5 to 8.8 MeV [2–5]. The binding energy per nucleon rises slightly with increasing mass number and reaches a maximum value for ^{62}Ni. Thereafter the binding energies decline slowly with increasing mass number. The

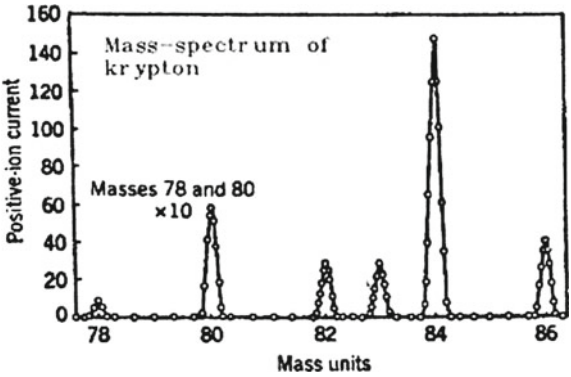

Fig. 2.4 A mass-spectrum analysis of krypton. The ordinates for the peaks at mass positions 78 and 80 should be divided by 10 to show these peaks in their true relation to the others (after [5])

binding energies of the atoms of H, He, Li and Be are lower than the binding energies of the other elements (see, also Fig. 2.5 below).

The measurement of nuclear masses occupies an extremely important place in the development of nuclear physics. Mass spectrometry (see, e.g. [66, 67]) was the first technique of high precision available to the experimenter, and since the mass of a nucleus increases in a regular way with the addition of one proton or neutron. In mass spectrometers, a flux of identical nuclei (ions), accelerated (see, e.g. Fig. 3.13 in [14]) to a certain energy, is directed to a screen (photoplate) where it makes a visible mark. Before striking the screen, this flux passes through magnetic field, which is perpendicular to velocity of the nuclei. As a result, the flux is deflected to certain angle. The greater mass, the smaller is the angle. Thus, measuring the displacement of the mark from the center of the screen, we can find the deflection angle and then calculate the mass. The example of a *mass-spectrum* of a different isotopes of krypton is shown in Fig. 2.4. From the relative areas of the peaks it can be determine the abundance of the stable isotopes of krypton (for details see [65]).

Relative masses of nuclei can also be determined from the results of nuclear reactions or nuclear decay. For example, if a nucleus is *radioactive* and emits an *α-particle*, we know from energy conservation that it mass must be greater than that of decay products by the amount of energy released in the decay. Therefore, if we measure the latter, we can determine either of the initial or final nuclear masses if one of them is unknown. An example of this is presented briefly below. At present we shall illustrate some typical reactions, bridging the gap between "classical" methods and the more advanced "high-energy" types of experiments (see, also [7, 61]).

The possible, natural *decay processes* can also be brought into the class of reaction processes with the conditions: no incoming light particle α and $Q > 0$. We list them in the following sequence:

α - decay:

$$ {}^{A}_{Z}X_{N} \rightarrow {}^{A-4}_{Z-2}Y_{N-2} + {}^{4}_{2}He_{2}. \tag{2.5} $$

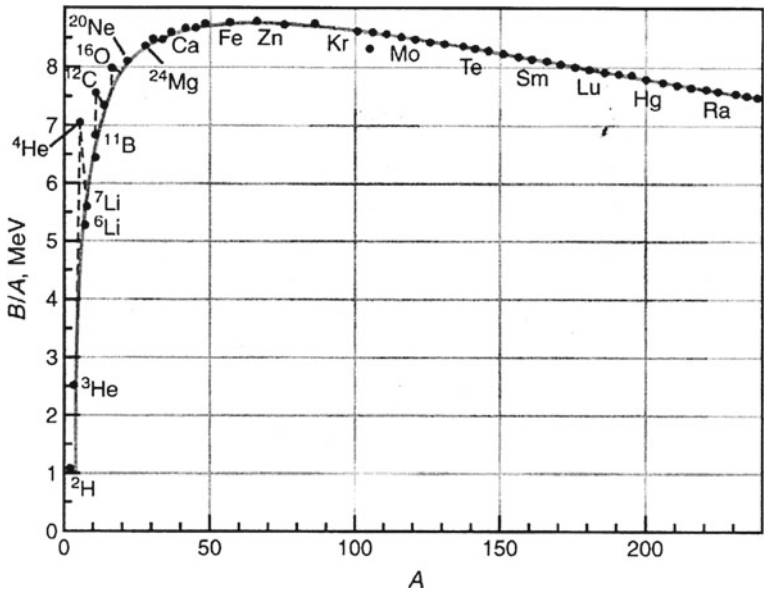

Fig. 2.5 The binding energy per nucleon B/A as a function of the nuclear mass number A (after [41])

β - decay:

$$^{A}_{Z}\mathrm{X}_{N} \rightarrow ^{A}_{Z-1}\mathrm{Y}_{N+1} + \mathrm{e}^{+} + \nu_e \quad (p \rightarrow n\text{-}type) \tag{2.6}$$

$$^{A}_{Z}\mathrm{X}_{N} \rightarrow ^{A}_{Z+1}\mathrm{Y}_{N-1} + e^{-} + \overline{\nu}_e \quad (n \rightarrow p\text{-}type) \tag{2.6'}$$

$$^{A}_{Z}\mathrm{X}_{N+\mathrm{e}^-} + \mathrm{e}^{-} \rightarrow ^{A}_{Z-1}\mathrm{Y}_{N+1} + \nu_e \quad (\mathrm{e}^{-}\text{-capture}). \tag{2.6''}$$

Here e^{-}, e^{+}, ν_e and $\overline{\nu}_e$ are electron, positron, neutrino and antineutrino.

γ - decay:

$$^{A}_{Z}\mathrm{X}^{*}_{N} \rightarrow ^{A}_{Z}\mathrm{X}_{N} + h\nu. \tag{2.7}$$

Here X* is excited nuclei.

Nuclear fission:

$$^{A}_{Z}\mathrm{X}_{N} \rightarrow ^{A_1}_{Z_1}\mathrm{Y}_{N_1} + ^{A_2}_{Z_2}\mathrm{U}_{N_2} + x \times n. \tag{2.8}$$

Table 2.5 Masses of electron, nucleons and some nuclei (after [41])

Particle	Number of Protons	Number of Neutrons	Mass (MeV)
e	0	0	0.511
p	1	0	938.2796
n	0	1	939.5731
$^{2}_{1}$H	1	1	1876.14
$^{3}_{1}$H	1	2	2808.920
$^{3}_{2}$He	2	1	2808.391
$^{4}_{2}$He	2	2	3728.44
$^{7}_{3}$Li	3	4	6533.832
$^{9}_{4}$Be	4	5	8392.748
$^{12}_{6}$C	6	6	11174.860
$^{16}_{8}$O	8	8	14895.077
$^{238}_{92}$U	92	146	221695.831

Since mass and energy are equivalent (see Einstein formula above), in nuclear physics it is customary to measure masses of all particles in the units of energy (MeV). Examples of masses of subatomic particles are given in Table 2.5.

As it was noted above, nuclear binding energy increases with the total number of nucleons A and, therefore, it is common to quote the average *binding energy* per nucleon (B/A) The variation of B/A with A is shown in Fig. 2.5. Several remarkable features are immediately apparent. First of all, the curve is relatively constant except for the very light nuclei. The average binding energy of most nuclei is, to within 10%, about 8 MeV per nucleon. Second, we note that the curve reaches peak near A = 60, where the nuclei are most tightly bound and light and very heavy nuclei contain less bound nucleons. Thus, the source of energy production in fusion of light nuclei or fission of very heavy nuclei can be a source of energy [13, 14].

While concluding this paragraph we should remember that it is often stated ^{56}Fe is the most tightly bound nucleus, but this is not correct since ^{62} Ni is more bound by a difference of 0.005 MeV/nucleon (for details see [68, 69] and references therein). In conclusion, it is very interesting to note that one cubic millimeter of *nuclear material*, if compressed together, would have a mass around 200,000 tonnes. *Neutron stars* are composed of such material.

As shown above nuclei vary from about one to a few fermis in radius. Recall that the Bohr radius of hydrogen is in the order 10^{-10} meters , so the nucleus at present time, despite its small size the nucleus has about, as was noted above, 99.9% of the mass of the atom (see, also [2, 3]). Electron scattering off nuclei is, for example, one of the most appropriate methods to deduce radii. The results of this procedure for several different nuclei are shown in Fig. 2.6. One remarkable conclusion is obvious—the central nuclear charge density is nearly the same for all nuclei. *Nucleons* do not congregate near the center of the nucleus, but instead have a fairly constant distribution out to the surface. The conclusion from measurements of the nuclear matter distribution is the same [70, 71]. Under this assumptions of saturation and

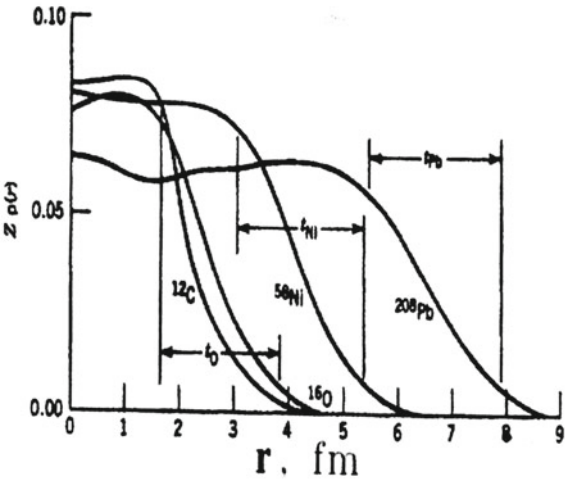

Fig. 2.6 The radial charge distribution of several nuclei determined from electron scattering. The skin thickness value t is roughly constant at 2.3 fm. The central density changes very little from the lightest nuclei to the heaviest (after [70, 71])

charge independence each nucleon occupies an almost equal size within the nucleus. Calling r_0 an elementary radius for a nucleon in the nucleus, a most naive estimate gives for the nuclear volume

$$\mathrm{V} = 4/3\pi r_0^3 \mathrm{A} \tag{2.9}$$

or

$$\mathrm{R} = r_0 \mathrm{A}^{1/3}. \tag{2.10}$$

This relation describes the variation of the nuclear radius, with value of $r_0 \simeq 1.2$ fm when deducing a "charge" radius and a "value of $r_0 \simeq 1.4$ fm for the full matter" radius (see also Figs. 3.5 and 3.9 in [5]). In a simple way the nuclear radius is defined as the distance at which the effect of the nuclear potential is comparable to that of the Coulomb's potential (see Fig. 2.7).

We should indicate another way to determine the nuclear charge radius from direct measurement of the Coulomb's energy differences of nuclei. Consider, for example, ${}^3_1\mathrm{H}_2$ and ${}^3_2\mathrm{He}_1$. To get from ${}^3\mathrm{He}_1$ to ${}^3\mathrm{H}_1$ we must change a proton into a neutron. As we know, there is strong a evidence which suggests that the nuclear force does not distinguish between protons and neutrons. Changing proton into a neutron should therefore not affect the nuclear energy of the three nucleon system: only the Coulomb's energy should change, because the two protons in ${}^3\mathrm{He}_1$ expexperience a repulsion that is not present in ${}^3\mathrm{H}$. The energy difference between ${}^3\mathrm{He}$ and ${}^3\mathrm{H}$ is thus a measure of the Coulomb's energy of the second proton, and the usual formula for the Coulomb's repulsion energy can be used to calculate the distance between the protons and thus the size of the nucleus.

The interactions between two nucleons (NN) is one of the central questions in physics and its importance goes beyond the properties of nuclei. Nucleons can combine to make four different few-nucleon systems, the deuteron $(p + n)$, the triton

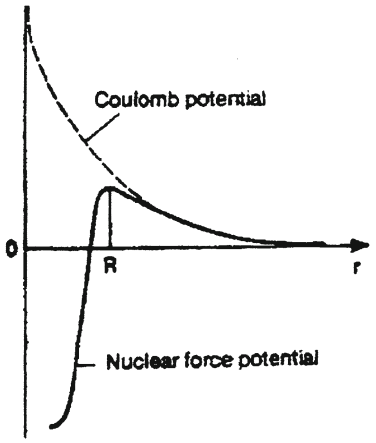

Fig. 2.7 Coulomb's potential used for defining the nuclear radius R

$(p + 2n)$, the helion $(2p + n)$ and the α-particle $(2p + 2n)$ (see, e.g. [72–75]). These particles are grouped together because they are stable (excluding from the radioactive triton which has a half-life of about 12 years and so may be treated as a stable entity for most practical purpose), have no bound excited states (except the α-particles which has two excited states at about 20 and 22 MeV) and are frequently used as projectiles in nuclear investigations. The absence of stable particles of mass of five provides a natural boundary between few-nucleon systems and heavier nuclei [38–40, 74]. Few nucleon systems provide the simplest systems to study nuclear structure. The *deuteron* provides important information about the nucleon–nucleon interaction.

Even before describing any further experimental and theoretical results to study the force between two nucleons, we can already guess at a few of the properties of the N–N force:

1. At short distances it is stronger than the *Coulomb's force*; the nuclear force can overcome the Coulomb's repulsion (see also Fig. 2.7) of protons in the nucleus.
2. At long distances, of the order of atomic sizes, the nuclear force is negligibly feeble. The interaction among nuclei in a molecule can be understood based only on the Coulomb's force.
3. Some fundamental particles are immune from the nuclear force. At present time we have not any evidence from atomic structure, for example, that electrons feel the nuclear force at all.
4. The N–N force seems to be nearly independent of whether the nucleons are neutrons or protons. As is well known this property is called *charge independence*.
5. The N–N force depends on whether the spins of the nucleons are parallel or antiparallel.
6. The N–N force includes a repulsive term, which keeps the nucleons at a certain average separation.

Table 2.6 Table of main families of particles

Family	Particle	Fundamental
Lepton	Electron	Yes
Lepton	Neutrino	Yes
Hadron	Proton	No
Hadron	Neutron	No
Hadron	Delta	No
Hadron	Sigma	No
Hadron	Many	More

7. The N–N force has a noncentral or *tensor component*. This part of the force does not conserve orbital angular momentum, which is a constant of the motion under central forces.

We should add that with knowledge of the N–N interaction provided by *p–p* and *p–n* scattering and by the deuteron [76–78] one can try to calculate the properties of the triton and the helion. The principal properties of few-nucleon systems are summarized in Table 2.6.

Deuteron. The *deuteron* is a very unique nucleus in many respects. It is only loosely bound, having a binding energy much less than the average value ($\leq$8 Mev [38–40]) between a pair of nucleons in all other stable nuclei. We have seen in Eq. (2.4) that the binding energy E_B of a nucleus is given by the mass difference between the neutral atom and the sum of the masses of free neutrons and protons in the form of hydrogen atoms. For a deuteron, as we can see from Table 2.5, the mass M_d is 1876.1244 Mev/c^2. The binding energy is then the difference between M_d and the sum of those for a neutron m_n and a hydrogen atom $m_H (=m_p)$: $m_n c^2 = 939.565$; $m_H c^{2=938.7833}$ MeV and $m_n + m_H = 1878.3489$ MeV. We can write according Eq. (2.4): $E_B = m_n + m_H - M_d = 2.224$ MeV. A more precise value, $E_B = 2.22457312$ MeV is obtained from radioactive capture of a neutron by hydrogen. In this reaction $p(n, \gamma)d$, a slow neutron is captured by a hydrogen atom followed by the emission of a γ-ray (for details see [79]).

To simplify the analysis of the deuteron *binding energy*, we will assume that we can represent the N–N potential of 3-D square well, as shown in Fig. 2.8

$$\begin{aligned} V(r) &= -V_0, \quad \text{for } r < R \quad (=2.1\text{fm}) \\ &= 0, \quad \text{for } r > R. \end{aligned} \tag{2.11}$$

This is of course an oversimplification, but is sufficient for at least some qualitative conclusions. In Eq. (2.11) r represents the separation between the proton and the neutron, so R is in effect a measure of the diameter of the deuteron (Fig. 2.9). If we express the energy, corresponding to the ground state value $E = -E_B$, the Schrodinger equation becomes for the 1-D, radial problem with zero angular moment, just like the lowest energy state of hydrogen atom.

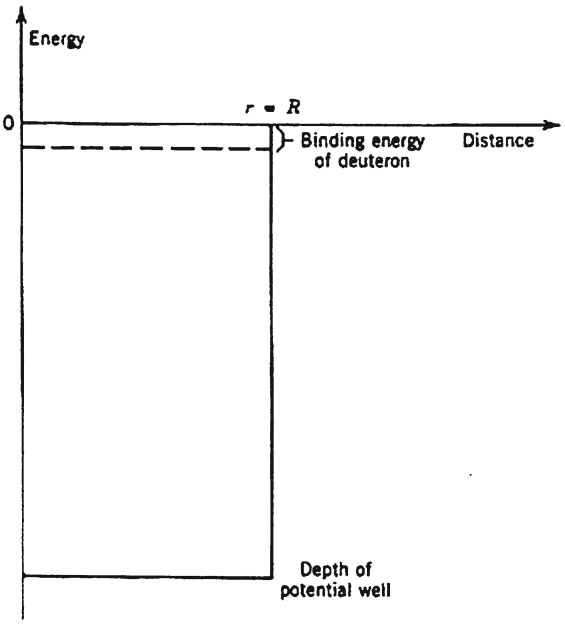

Fig. 2.8 The spherical square-well potential, adjusted to describe correctly the binding energy E_B of the deuteron. The full depth is also given and amounts to $V_0 = U = 38.5$ MeV (after [41])

$$\begin{aligned} &\frac{d^2u}{dr^2} + k^2u = 0, \quad r < R \text{ (see, Fig. 2.8)} \\ &\frac{d^2u}{dr^2} - \alpha^2 u = 0, \quad r > b, \end{aligned} \tag{2.12}$$

defining

$$k^2 = \frac{m_n}{\hbar^2}(u - E_B), \quad \alpha^2 = \frac{m_n}{\hbar^2}E_B \tag{2.13}$$

and using the radial solution

$$u(r) = rR(r). \tag{2.14}$$

Approximate solutions in the two regions became

$$\begin{aligned} u(r) &= A\sin kr, \quad r < R \quad \text{and} \\ u(r) &= Be^{-\alpha(r-R)} \quad r > b. \end{aligned} \tag{2.15}$$

Matching the logarithmic derivatives at $r = R$ gives

$$k\cot anKr = -\alpha \tag{2.16}$$

and matching the wave functions at $r = R$ gives

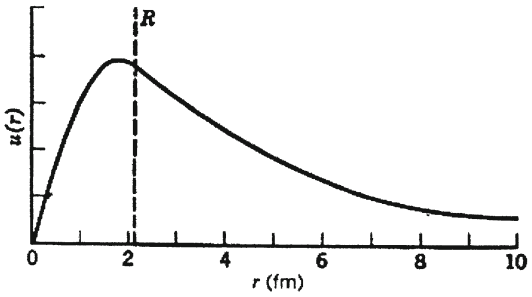

Fig. 2.9 The deuteron wave function for R = 2.1 fm (after [5])

$$\mathrm{AsinkR} = B. \tag{2.17}$$

These two relations lead to the condition

$$k^2\mathrm{A}^2 = (k^2 + \alpha^2)\mathrm{B}^2. \tag{2.18}$$

The normalization of the wave function $4\pi \int u^2(r)\mathrm{dr} = 1$ becomes

$$\frac{\mathrm{A}^2}{2k}(2kR - \sin 2kR) + \frac{\mathrm{B}^2}{\alpha} = \frac{1}{2\pi}. \tag{2.19}$$

Eliminating A^2 from the last two equations, gives the value for B as

$$B \simeq \sqrt{\frac{\alpha}{2\pi}}\mathrm{e}^{-\alpha \mathrm{R}/2}. \tag{2.20}$$

Knowing the *binding energy* E_B [see, Eq. (2.13)], we can determine the value $\alpha = 0.232\ \mathrm{fm}^{-1}$. A best value for R can be determined from proton–neutron scattering (see, e.g. [72–74]) as $R = 1.93$ fm. This then gives u = 38.5 MeV. One can show that this value of u and the value for R just give rise to a single, bound $1s$ state, all other higher-lying $1p$, $1d$, $2s$ being unbound. Since we also have

$$\mathrm{A} \simeq \mathrm{B} \tag{2.21}$$

we obtain the final wave functions

$$\begin{aligned} u(r) &= \sqrt{\tfrac{\alpha}{2\pi}}\mathrm{e}^{-\alpha \mathrm{R}/2}\sin \mathrm{kr}, \quad r < \mathrm{R} \quad \text{and} \\ u(r) &= \sqrt{\tfrac{\alpha}{2\pi}}\mathrm{e}^{-\alpha \mathrm{R}/2}\mathrm{e}^{-\alpha \mathrm{r}} \quad r > \mathrm{b} \end{aligned} \tag{2.22}$$

A potential which gives a satisfactory account of the properties of the deuteron given in Table 2.7 is shown in Fig. 2.10. We should add that in all deuteron potentials the *tensor term* is a very sizeable part of the two-nucleon potential, and is charac-

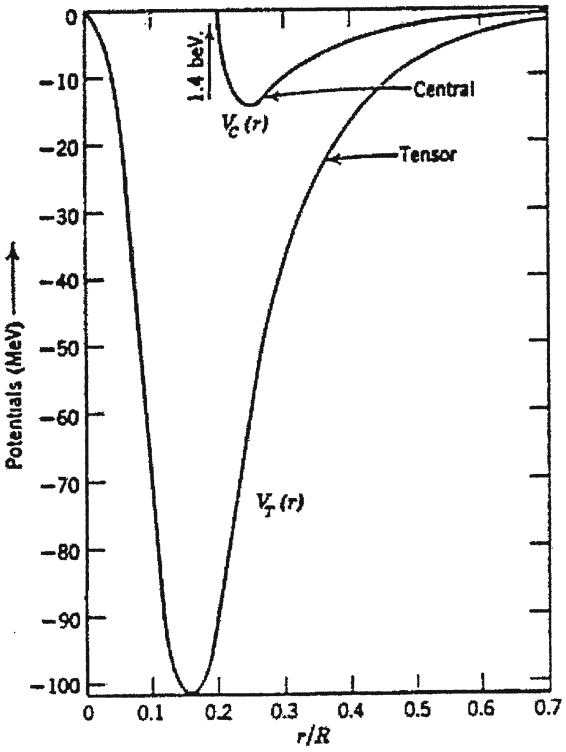

Fig. 2.10 The potential for deuteron triplet states with even L. the distance is in units of deuteron radius R = 4.31 fm (after [80])

terised by a somewhat larger range than the central potential (see Fig. 2.10) being appreciably different from zero even when the central potential is already negligible.

Proton–proton and proton–neutron interactions. Most of the present theories (see, also [74] and references therein) of *nuclear structure* and nuclear reactions are based on the assumption that nuclear properties depend mainly on *two-body interactions* between its constituents. Three-body forces or many-body forces are expected to play only a minor role.[4] It is thus of paramount importance to describe as accurately as possible the two-nucleon interaction. At the fundamental level this interaction is a consequence of the quark structure of the nucleons and should be described by QCD [75] in terms of the quark-gluon field (see, also [54–56, 72, 82]).

However this approach is still in its infancy and therefore we are still far from solution. There are also many indications [72, 73] that at interaction energies below a few hundred MeV it is possible to describe the N–N interaction in terms of the exchange of various types of mesons [83–86].

[4] If the two-body potential has an average strength of 20 MeV, then the three-body one would have a strength of about 1 MeV. We should add that all models have a one-pion exchange character at long range, which gives rise to a spin–spin central potential and a tensor term (for details see [60, 81]).

In principle there are four types of scattering measurements involving two nucleons that can be carried out. The scattering of an incident proton off a proton (*pp-scattering*) is the simplest one of the four from an experimental point of view, as it is relatively easy to accelerate protons and to construct targets containing hydrogen. For *neutron scattering*, there are two major sources for incident beam. At low energies, neutrons from nuclear reactors may be used. At higher energies, one can make use of neutrons produced by a beam of protons, for instance, through a (*p, n*) reaction on a ^{7}Li target. However, both the intensity and the energy resolution of neutron beams obtained in these ways are much more limited than those for proton beams. As a result, neutron scattering is, in general, a more difficult experiment than those with protons. In addition to *pp*- and *np*-measurements, one can, in principle, carry out *pn*- and *nn*-scattering experiments as well. Here, instead of using protons as the target, a neutron target is used. As we know, free neutrons are unstable (see above), with a half-life in the order of 10 min. It is therefore impossible to construct a fixed neutron target, in contrast to protons where material consisting of hydrogen may used. There are, in principle [84, 85], two methods of getting around this limitations. One way is to carry out a colliding beam experiment. In place of a target fixed in the laboratory, a second neutron beam is used and, instead of having an incident beam scattering from a fixed target, two beams of particles are directed towards each other. Scattering takes place when the particles in the two beam collide. To be practical, such an experiment requires high intensities in both beams, and currently highly intense beams of neutrons are not easily available. The other way is to simulate a fixed neutron target using deuterium. Since the deuteron is a loosely bound system of a neutron and a proton, the desired *pn*- or *nn-scattering* results can be obtained by carrying out the corresponding *pd*- or *nd*-scattering experiments. The contribution due to protons in the deuterium target may be removed by subtracting from the measured values the corresponding results obtained in *pp*- or *np*-scattering. The information obtained from *pn*- and *nn*-scattering may not be different from that in *np*- and *pp*-scattering. For example, the only difference between *pn*- and *np*-scattering is whether the neutron or the proton is the target. Under time-reversal invariance, these two arrangements are expected to give identical results. As early to simplify the notation, we shall use the symbol NN from now on to represent a system of two nucleons, as early, when there is no need to differentiate between neutrons and protons and the symbol *np* to represent both *np*- and *pn*-unless further distinction is required by the occasion. Futhermore, we shall assume that *Coulomb's contribution* where present, has already been taken out and we can therefore ignore it in the discussion.

The quantity measured in a scattering experiment is the number of counts registered by a *detector* (θ, φ) (see, e.g. [68]). The counting rate depends on the solid angle subtended by the detector at the scattering centre, the intensity of the incident beam, the number of target nuclei involved and the differential cross-section $\mathrm{d}\sigma/\mathrm{d}\Omega$. Naturally, our primary interest is in $\mathrm{d}\sigma/\mathrm{d}\Omega$, a function of the bombarding energy as well as the scattering angle. For simplicity we shall consider first only *elastic scattering*, and as a result, the wave number k in the centre of mass of the two particles has the same magnitude before and after the scattering. The differential scattering *cross-section* at angles (θ, φ) is given by next equation

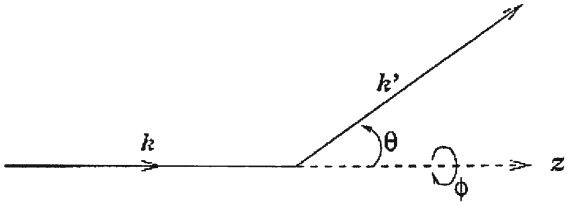

Fig. 2.11 Schematic diagram of a scattering arrangement. The scattering angle θ is between wave vector $\overrightarrow{k}$, along the direction of the projectile, and $\overrightarrow{k}'$, that of the scattered particle. The result is independent of the azimuthal angle Φ unless the orientation of the spin of one of the particles involve d is known (details see in text)

$$\frac{\mathrm{d}\sigma}{\mathrm{d}\Omega}(\theta, \varphi) = |f(\theta, \varphi)|^2 . \tag{2.23}$$

Here $f(\theta, \varphi)$ is the *scattering amplitude*. As shown in Fig. 2.11 the geometry of 0-scattering arrangement is such that it is coordinate system at the centre of the scattering region and takes the direction of the incident beam as the positive direction along the z-axis. The incident wave vector $\overrightarrow{k}$ and the scattered vector $\overrightarrow{k}'$ define a plane, the scattering plane.

For a *central potential*, the relative angular momentum $\overrightarrow{l}$ between the two scattering nucleons is a conserved quantity. Under such conditions, it is useful to expand the wave function as a sum over the contributions from different partial waves, each with a definite l-value

$$\Psi(r, \theta) = \sum_{l=0}^{\infty} a_l Y_{l0}(\theta) \mathrm{R}_l(k,\ r). \tag{2.24}$$

Here a_l is the expansion coefficients. Only spherical harmonics $\mathrm{Y}_{lm}(\theta, \varphi)$ with $\mathrm{m} = 0$ appears in the expansion since, in the absence of polarization, the wave functions is independent of the azimuthal angle Φ. We have explicitly included the wave number k in the arrangement of the radial wave function $\mathrm{R}_l(k,\ r)$ so as to emphasise the dependence of energy.

For a free particle, $V = 0$, and the radial wave function reduces to

$$\mathrm{R}_l(k,\ r) \to \frac{1}{kr} \sin\left(kr - \frac{1}{2} l\pi\right), \tag{2.25}$$

where $k = \sqrt{2\mu \mathrm{E}}/\hbar$ and $\mathrm{j}_l(\rho)$ is the spherical Bessel function of the order l. If only elastic scattering is allowed by the potential, the probability current density in each partial-wave channel is conserved. The only effect the potential can have on the wave

function is a change in the phase angle. In other words

$$\mathrm{R}_l(k,\ r)(\mathrm{scatt/r} \to \infty) \to \frac{1}{\mathrm{kr}} \sin\left(\mathrm{kr} - \frac{1}{2}\mathrm{l}\pi + \delta_\mathrm{l}\right), \tag{2.26}$$

where δ_l is the phase shift in the lth partial-wave channel.

After that, the scattering amplitude may be expressed in terms of δ_l as

$$f(0) = \frac{\sqrt{4\pi}}{k} \sum_{l=0}^{\infty} \sqrt{2l+1}\mathrm{e}^{i\,\delta_i} \sin\delta_l \mathrm{Y}_{l0}(\theta). \tag{2.27}$$

In such case the differential scattering cross-section may be written in terms of the phase shift

$$\frac{\mathrm{d}\sigma}{\mathrm{d}\Omega} = \frac{4\pi}{k^2} \left| \sum_{l=0}^{\infty} \sqrt{2l+1}\mathrm{e}^{i\,\delta_i} \sin\delta_l \mathrm{Y}_{l0}(\theta) \right|^2. \tag{2.28}$$

The scattering cross-section, the integral of $\frac{\mathrm{d}\sigma}{\mathrm{d}\Omega}$ over all solid angles, becomes

$$\sigma = \int \frac{\mathrm{d}\sigma}{\mathrm{d}\Omega} d\Omega = \frac{4\pi}{k^2} \sum_{l=0}^{\infty} (2l+1)\sin^2\delta_l(k). \tag{2.29}$$

Decomposition into partial waves is a useful way to analyse the scattering results for a given bombarding energy. In particular, only a few of the low-order partial waves can contribute to the scattering at low energies, as shown in Fig. 2.12. For realistic *nuclear potential*, the orbital angular momentum is not conserved.

Since we are dealing with identical fermions, the scattering of two nucleons can take place only in a state that is totally *antisymmetric* with respect to a *permutation* of the two particles, in the same way as for deuteron. For *pp*-sattering, we have $\mathrm{T} = 1$ [5] and the two nucleons are symmetric, as for their total isospin wave function [60] is concerned. If the intrinsic spins of the two protons are coupled together to $\mathrm{S} = 0$ (antisymmetric state) and, as a result only even l-values are allowed. For $\mathrm{S} = 0$, we have $\mathrm{J} = \mathrm{l}$ (we remind that $\vec{J} = \vec{l} + \vec{S}$), and the partial waves for the lowest two orders of *pp*-scattering are $^1\mathrm{S}_0$ ($\mathrm{l} = 0$) and $^1\mathrm{D}_2$ ($\mathrm{l} = 2$). The phase shifts extracted from measured *pp*-scattering data for these two partial waves of bombarding energy less than 300 MeV, in the laboratory are shown in Fig. 2.13 as illustrative examples (for details see [87]). Only the real part of the phase shift is given. At laboratory energy less than 300 MeV, contributions from inelastic scattering are still relatively

[5] In 1932 Heisenberg suggested [90] on the basis of the approximate of the proton and neutron mass (see also Table 2.2) that these particles might be considered as two different charge states of a single entity, the *nucleon*, formally equivalent to the up and down states of a spin 1/2 particle. To exploit this hypothesis the nucleon wave function in addition to a space and a spin component also has an isotopic spin (isospin) component (see, also e.g. [7]).

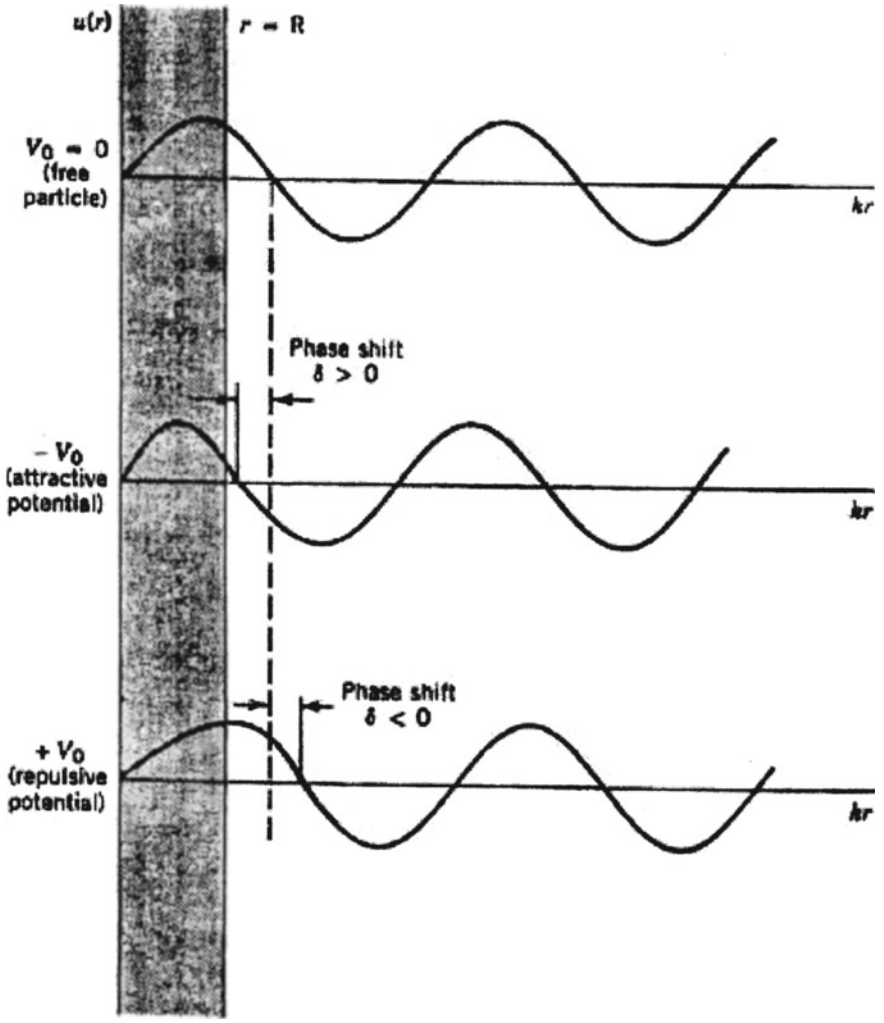

Fig. 2.12 The effect of a scattering potential is to shift the phase of the scattered wave at points beyond the scattering regions, where the wave function is that of a free particle (after [6])

unimportant and the imaginary parts of the phase shifts extracted from measured scattering cross-section are small (see Table 2.8).

By the same token, partial waves for triplet (S = 1) *pp-scattering* have odd l-values. The lowest order in this case is a p-wave ($l = 1$). When $l = 1$ is coupled with S = 1, three states with J = 0, 1, 2 are produced. The phase shifts for two of the triplet of states, $^3P_0$ and $^3P_1$, are also shown in Fig. 2.13a. There is no admixture between the two J = 0 states $^3P_0$ and $^1S_0$, as they are of different parity. As a result

Table 2.7 Properties of nucleons and few-nucleons systems

Particle	Symbol	Spin	Parity	BE(MeV)	MM (μ_0)	QM(fm^2)	RMS CR(fm)
Proton	p	1/2	+		$2.79284739\pm6\times10^{-8}$		0.88
Neutron	n	1/2	+		$-1.9130428\pm5\times10^{-7}$		
Deuteron	^{2}H	1	+	2.2246	$0.8574376\pm4\times10^{-7}$	0.288 ± 10^{-3}	1.963
Triton	^{3}H	1/2	+	8.482	2.978960 ± 10^{-6}		1.63±0.03
Helion	^{3}He	1/2	+	7.718	$-2.127624\pm1.12\times10^{-6}$		1.97±0.0015
Alpha	^{4}He	0	+	28.28			1.671±0.014

Here *BE* binding energy, *MM* magnetic moment, *QM* quadrupole moment; *RMS CR* RMS charge radius

Table 2.8 Nucleon–nucleon scattering length (a) and effective range (r_e)

	$s=0; T=1$ (fm)	$s=1; T=0$ (fm)
pp: a	−17.1±0.2	
pp: r_e	2.794±0.015	
nn: a	−16.6±0.6	
nn: r_e	2.84±0.03	
np: a	−23.715±0.15	5.423±0.005
np: r_e	2.73±0.03	1.73±0.02

we find that both l and S are good quantum numbers here by default (for details see [89] and references therein and Table 2.8).

The *np*-system may be coupled together to either isospin T = 0 or T = 1. For T = 0 the two nucleons are antisymmetric in *isospin*. In this case the S = 0 states must have odd l-values in order to be antisymmetric in the total wave function. The lowest order partial wave here is l = 1 and the phase shifts for ^{1}P$_1$-scattering extracted from experimental data are shown in Fig. 2.13c. In order for p-wave *np*-scattering to be in the S = 1 state, it is necessary for the total isospin to be T = 1. The phase shift in this case is expected to be identical to those found in *pp*-scattering, if nuclear force is charge independent and *Coulomb's* effects are removed. An examination of the two sets of empirical *p*-wave phase shifts, ^{3}P$_0$ and ^{3}P$_1$ given in Fig. 2.13b, shows that they are only slightly different from corresponding values given in Fig. 2.13a for *pp*-scattering. It is not clear whether the small differences come from the way the phase shifts are extracted from experimental scattering cross-section or they are indications of a weak charge dependence in the nuclear force (see, also Fig. 2.14).

The other T = 0 phase shift in the *np*-system, shown in Fig. 2.13c, is for triplet (S = 1), even *l*-scattering. This is the first time we encounter a mixing of different *l*-partial waves. Until now, each phase shift has been characterised by a definite *l*-value (as well as J- and S-values) even though the orbital angular momentum is not fundamentally a good quantum number. Mixing of different *l*-partial waves has not taken place because of parity and other invariance conditions; however, the tensor force can mix two triplet of the same J but different in l by two units ($l = J\pm1$) (see also [89]).

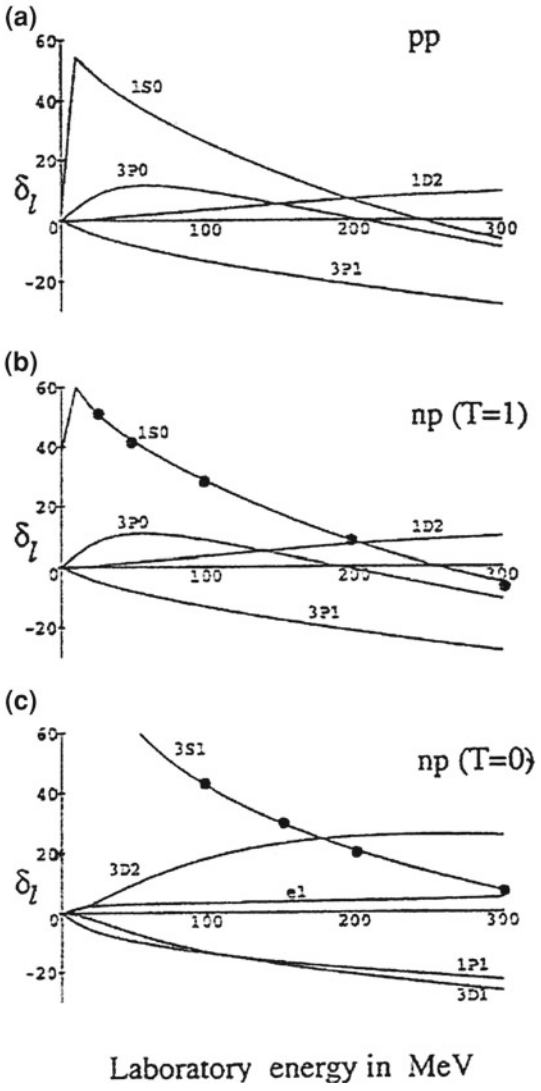

Fig. 2.13 Real part of NN-scattering phase shifts in degrees for low-order partial waves [87]: **a** *pp*-scattering with contribution from the Coulomb's potential removed. **b** isovector *np*-scattering, and **c** isoscalar *np* scattering. *Filled circles* in the $^1S_0$ and $^3S_1$ phase shifts of *np*-scattering are the calculated results using a Paris potential (after [88])

Our present knowledge of *nuclear physics* suggests that there are two main families of particles *leptons* and *hadrons* (*baryons* and *mesons*). The hadrons were first thought to be elementary like the leptons, but soon a very large number of hadrons were discovered, which suggest that they are not elementary (see, also [5, 70, 71, 91–93]). As we can see from Table 2.6 the leptons are fundamental particles, but hadrons are not. They are made up of *quarks* [94, 95] (for details see below). The hadron found in normal matter are the proton and the neutron. Quarks are one of the two basic constituents of matter which is described *QCD*. QCD [54–56, 96, 97] is

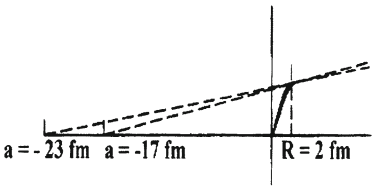

Fig. 2.14 Very small changes in the NN wave function near r = R can lead to substantial differences in the scattering length when the extrapolation is made (after [10])

Table 2.9 Characteristics of the quarks

Flavor	Electric charge (e)	Mass (GeV/c^2)
u—up	+ 2/3	0.004
d—down	− 1/3	0.008
c—charm	+ 2/3	1.5
s—strange	− 1/3	0.15
t—top	+ 2/3	176
b—beaty (bottom)	− 1/3	4.7

the theory of the strong interaction, a fundamental force describing the interactions of the quarks and gluons found in nucleons such as the proton and the neutron. QCD is an important part of the *Standard Model* (SM)[6] of particle physics (see, also [96, 97]). In the present SM [54–56] there are six "flowers" of quarks (see, below Table 2.9) most familiar baryons are the proton and neutron, which are each constructed up and down quarks [82, 98, 91]. Quarks are observed to occur only in combination of two quarks (mesons), three quarks (baryons), and the recently discovered with five quarks (pentiquarks [82]).

(a) *Quarks.* We now know that all the known properties of the hadrons (their quantum numbers, mass, charge, magnetic moment), their excited states and their decay properties (see, also below) may be explained by assuming that the mesons are made of quark–antiquark pairs, the baryons of three quarks and the antibaryons of three antiquarks [82, 96, 97]. To obtain this picture we need six quarks: *up*(u), *down* (d), *charm* (c), *strange* (s), *top* (t) and *bottom* (*beauty*) (b) (see Table 2.9). These six particles may be arranged according to their masses into three pairs, with one number of each pair having a charge +2/3e and the other −1/3e as shown in Table 2.9.Since quarks have not been observed in isolation, they appear either as bound quark–antiquark[7] pairs in the form of mesons or bound groups in the form of

[6] As is well known, the Standard Model [48–52, 54–56, 97, 81, 100] is a unified gauge theory of the *strong*, *weak* and *electromagnetic interactions*, the content of which is summarised by the group structure SU(3)× SU(2)× U(1), where SU(3) refers to the theory of strong interactions,QCD, and latter two factors [SU(2)× U(1)] describe the theory of electroweak interactions. Although the theory remains incomplete, its development represents a triumph for modern physics (for details see [100] and below).

[7] The first question that occurs is whether the quarks actually exist inside the hadrons or whether they are merely a convenient mathematical ingredient leading to the geometrical symmetry [7]. A substantial clue in this direction is obtained in deep inelastic scattering from nucleons [11–13]. The

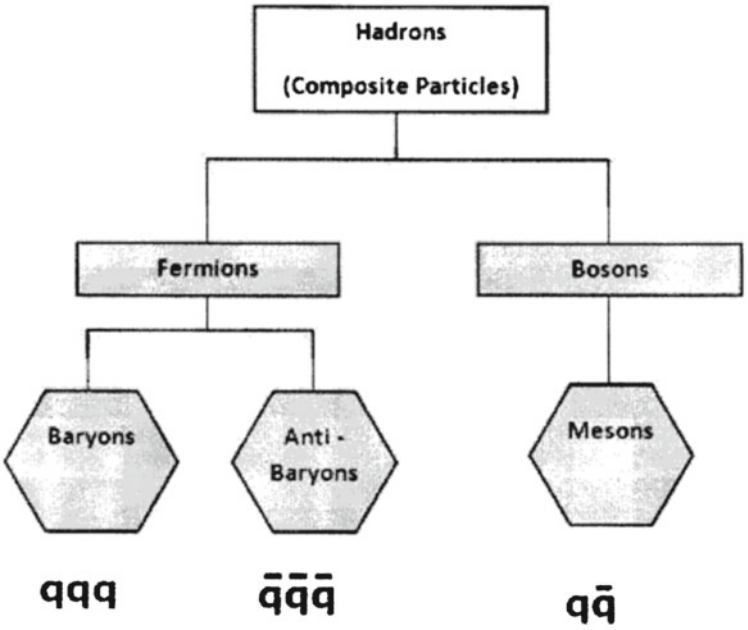

Fig. 2.15 Building blocks of matter, fermions have three quarks qqq and antiquarks $\overline{q}q\overline{q}$ as well as bosons are quarks and antiquarks

baryons (see, also Fig. 2.15)—the name assigned to them, up, down, strange, etc., are only mnemonic symbols to identify of different species. The word "flavour" is used, for convenience, to distinguish between different types of quark. Besides flavour, quarks also come in three different colours, for example, red, green and blue. Colour and flavour are quantum-mechanical labels, or in other words, quantum numbers, very similar to spin and parity. Since there are no classical analogous to flavour and colour degrees of freedom, there are no observables that can be directly associated with them. In this respect, they are similar to the parity label of a state which must be observed through indirect evidence.

Now we know that colour charge is the charge associated with *strong interaction*. Colour is whimsically named attribute of *quarks* and *gluons* [109] that cannot be seen. Gluons have one colour and one anticolour [110, 111]. There are, however, only eight types of gluons [5], not nine as we might expect. Quarks and gluons are only found inside hadrons. The quarks inside a hadron are bathed in a sea of gluons

nucleon appears to be made up of to regions in the asymptotic-free regime [100–102] and the outer region of the meson cloud where pions and other heavy mesons can exist (see, also [103–108]). A number of early results on the internal proton structure became accessible through highly inelastic electron scattering carried out at the Stanford Linear Accelerator centre (SLAC). Later work of Kendell et al. [11–13] helped to identify these structures with quarks inside the proton (for details see also [109]).

(and additional quark–antiquark pairs) that are responsible for the binding forces in the hadron. Quarks continually emit and absorb gluons. Colour charge is conserved in every such process. The colour mathematics always work out so that at any instant the entire hadron system is colour neutral.

For quarks, the interaction is very strong at low energies where nuclear physics operates and where most of the experimental observations are made. Because of what is generally known as asymptotic freedom [100, 102], the quark–quark interaction is weak only at extremely high energies. As a result, perturbational techniques apply to *QCD* only at such extremes, far beyond the realm of nuclear physics and low-lying hadron spectroscopy. Since quarks are not observed in isolation, their mutual interaction must have a component that grows stronger as the distance of separation between them increases. This is opposite to our experience in the macroscopic world, where interactions, such as gravitational and electromagnetic, grow weaker as the distance of separation between the interacting objects is increased (and the relation is given by the inverse square low).

From the above text it has become clear that protons and neutrons are no longer considered as elementary (see, also Fig. 2.15) but are composed of quarks in a *bound state*. The binding forces are quite distinct from electromagnetic, gravitational forces: at very short distance, the quarks appear to move freely but, with increasing separation, the binding forces increase in strength too. So it is not possible to separate the nucleon into its constituent quarks.[8] From this picture is followed that quarks are to be able to exist only in combination with other quarks (baryons) or with antiquarks (mesons) [60, 109]. This picture has also modified our ultimate view of a system of densely packed nucleons. For composite nucleons, interpenetration will occur if the density is increased high enough and each quark will find many other quarks in its immediate vicinity (see Fig. 2.16). The concepts of a nucleon and of nuclear matter become ill-defined at this high-energy limit and a new state of matter might eventually be formed: a quark plasma whose basic constituents are unbound quarks [81, 110, 111]. Starting with the matter of vanishing baryon density, the energy density of a non-interacting gas of massless quarks and gluons is (see, also [118, 119])

$$\mathrm{E} \simeq 12\mathrm{T}^4, \tag{2.30}$$

Where T is temperature. Just like in the Stefan–Boltzman for a proton gas, the numerical factor in (2.30) is determined by the number of degrees of freedom of the constituent particles: their spins, colours and flavours. The energy density for quarks plasma via computer simulations is obtained in [81]. The transition temperature from the mesonic regime to the plasma regime is around 200 MeV which means an energy density of at least $2.5\,\mathrm{GeV\,fm^{-3}}$ in order to create a quark-gluon plasma.

As is well known, the neutron decay was thus written

[8] As we know, nonrelativistic quark model use *constituent quark* masses, which are of order 350 MeV for u- and d-quarks. Constituent quark masses model the effect of dynamical chiral symmetry breaking are not related to the quark mass parameters m_q of the *QCD* Lagrangian.

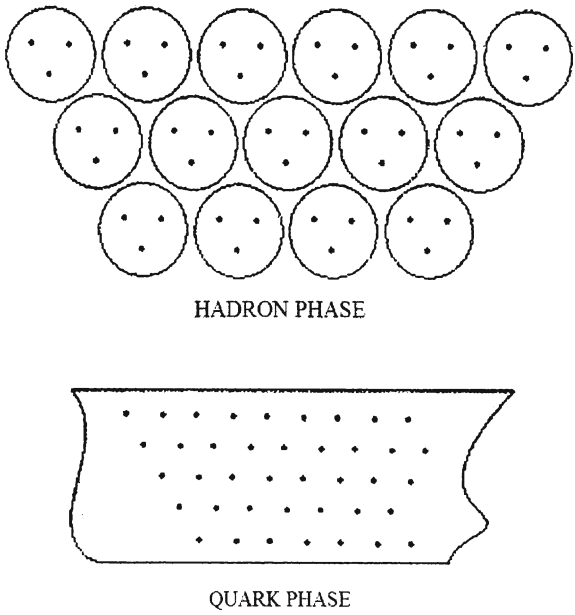

Fig. 2.16 Comparison of a collection in hadronic or nuclear matter phase and within quark-gluon plasma description (after [110, 111])

$$n \rightarrow p + e^{-} + \widetilde{\nu}_e, \tag{2.31}$$

where $\widetilde{\nu}_e$ is an electron antineutrino. This decay illustrates some of this conservation lows which govern particle decays.

The proton in the product satisfies the conservation of *baryon number*, not the emergence of the electron unaccompanied would violate conservation of lepton number. The third particle must be an electron antineutrino to allow the decay to satisfy lepton number conservation The electron has lepton number 1 and the antineutrino has lepton number -1. However, a proton bound in a nucleus may also transform into neutron by emitting a positron and a neutrino. This process is a bound as β^{+}-decay and discussed in any textbooks (see, e.g. [6, 7]). Also for this transformation the above consideration holds and the proton transformation into a neutron was written

$$p_{\text{bound}} \rightarrow n + e^{+} + \nu_e, \tag{2.32}$$

where ν_e is an *electron neutrino*. In conclusion of this part, we should note, that the *lepton number* conservation rule is applied to all cases it is found to work.

As we known well, at present time all *hadrons* are subdivided into two classes *baryons* and *mesons* (see Fig. 2.15). Baryons are distinguished by the fact that they are fermions, particles that obey Fermi-Dirac statistics. Because of this property, two baryons cannot occupy the same quantum-mechanical state. The fact that baryons are fermions implies that quarks must also be fermions, as it is impossible to construct fermions except from odd numbers of fermions. Furthermore, if we accept that a

quark cannot exist as a free particle, the lightest fermion in the hadron family must be made of three quarks (see also Fig. 2.15). Among the baryons, we are mostly concerned with the lightest pair, the neutron and the proton. From charge conservation alone, it can be deduced that a proton carrying a charge +e, must be made of two u-quarks, each having a charge of 2/3e (Table 2.9), and one d-quark, having a charge of −1/3e. The *quark wave function* of a proton may be represented as

$$| p >=| \text{uud} >. \tag{2.33}$$

Similarly, the quark wave function of a neutron is

$$| n >=| \text{udd} > \tag{2.34}$$

so that the total charge of a neutron in units of e is $2/3 - 1/3 - 1/3 = 0$.

Boson particles obeying Bose–Einstein statistics may be made from even number of fermions. This means that mesons are constructed of an even of quarks. Since, on the one hand, bosons can be created or annihilated under suitable conditions and, on the other hand, the number of quarks is conserved in *strong interaction* processes, a meson must be made of an equal number of *quarks* (see, also Fig. 2.15). The simplest meson is, therefore made of quark–antiquark. For example, pions (π), the lightest members among the mesons, are made of a quark, either u or d and an *antiquark*, either $\overline{u}$ or $\overline{d}$ (see, e.g. [109]).

2.3 Big Bang and Stellar Nucleosynthesis: Origin of Elements

The nuclear and particle physicists, the early *Universe*, represents the ultimate particle accelerator in which energies and densities of particles were beyond what we can ever hope to achieve with artificially constructed accelerators. Most modern views of cosmology are in agreement with the idea that the Universe began with an explosion, or "*Big Bang*" some 10–20 billions years ago. The uncertainties in the models are connected mostly with the very beginning of time, within the first fraction of a second or so. At the end of approximately the first 3 min. [112], and three-fourth of the baryon mass in the Universe is in the form of protons and the rest in the form of ^{4}He (see, e.g. [38–40]) Traces of deuteron, ^{3}He, and ^{7}Li are also present but their abundances are down by several orders for deuteron and ^{3}He and 10 orders for ^{7}Li (see, also Fig. 2.17).

Gamow [114–116] and Alpher and others [117] attempted to explain the relative abundance of all elements and isotopes from neutrons, following the hypothetical explosion which marked the beginning of the Universe (see, also [118, 119]). We now place this event $\sim 1.5 \times 10^{10}$ years ago. After that a number of modifications were made to the original theory. The first was made by Hayashi [120], who noted that at the high temperatures in the very early Universe, ther should be an equilibrium between protons and neutrons. The second modification was suggested by Fermi and

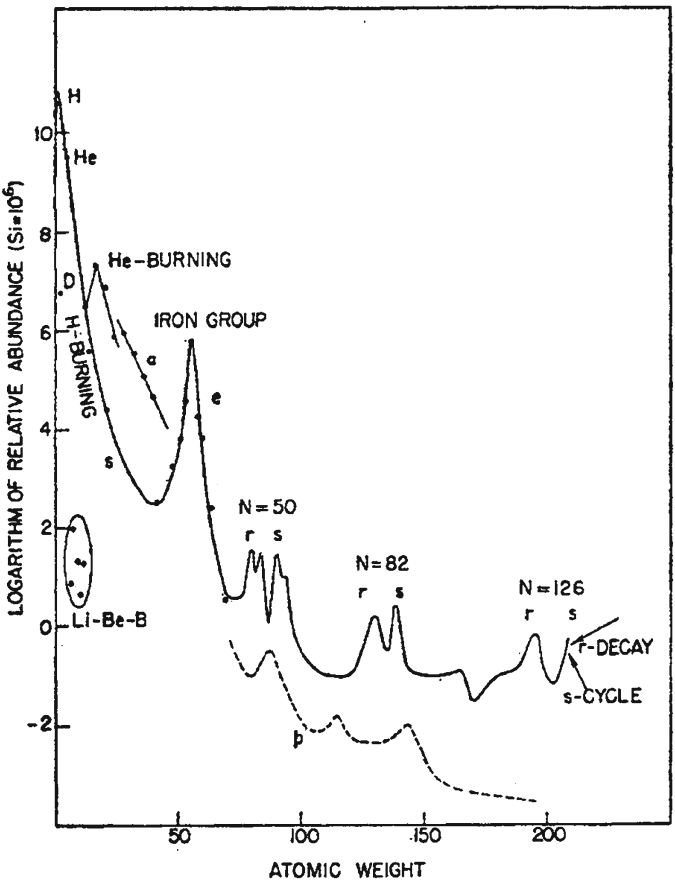

Fig. 2.17 Schematic curve of atomic abundance as a function of atomic weight based on data of Sues and Urey [113]. This author have employed relative isotopic abundance to determine the slope and general trend of the curve (after [113])

Turkevich [118, 119], who noted that lack of stable nuclei at mass 8 prevented the formation of carbon. As a result, this theory was neglected until the mid 1960s. Today the picture of the Big Bang is generally accepted, and forms on essential part of our understanding of the abundance of the elements (see [38]). The strongest facts in favour of the Big Bang theory are:

1. The relative abundance of the light elements [74].
2. The microwave background, which is remnant of the photon field of the Big Bang [121, 122].
3. The agreement of the ages of the oldest stars with the age of Universe.

The most convincing evidence for the Big Bang was provided by the discovery of the microwave background [121, 122]. Strong additional support for the *Big Bang*

model came from the conclusion by authors [124]. For review and history of this question see [125].

Temperature and densities in the Big Bang model are shown in Fig. 2.18. As the expansion began, temperature was too high to allow complex nuclei to survive. About 100s after the start of the Big Bang, T $\langle 1.3\times 10^9$ K (equivalent to an energy of 110 keV) (see, also [5, 8]). Then complex nuclei could survive, so the nucleosynthesis of light elements occur [74]; this is sometimes referred to as the era of nucleosynthesis. The modern theory of this process is referred to as standard Big Bang nucleosynthesis. About 3,000 years later, the expanding material cooled below $\sim 10^3$ K, so that hydrogen ions could recombine.

As was shown above, free *neutrons decay* into protons with a half-life of about 10 min. For a neutron to survive much longer time periods, it must be captured by other nucleons to form a bound nucleus. Since most of the nucleons in the *Universe* are in the form of free protons and neutrons at this stage, the most likely candidate to be formed is the deuteron, a bound nucleus made of a proton and a neutron. Unfortunately the binding energy of a deuteron is very small and this constitutes the major bottleneck in preserving primordial neutrons from β-decay. Because of the short range of nuclear force, bound nuclei can be made from free neutrons and protons only through random collisions that bring some of them into close contact with each other. The probability of such encounters drops drastically for three or more particles. This leaves us with deuteron as the only likely bound system that can be made in any significant amount. On the other hand, the small binding energy means that deuterons can also be destroyed easily in random collisions with other particles. The most likely event is with photons, as there is something like 10^9 for each nucleon. For this reason, photodisintegration constitutes an important sink for any deuterons created when the temperature is still sufficiently high. On further cooling, some deuterons can exist long enough to capture a proton to form ^{3}He. In turn, ^{3}He can capture a neutron and transform it into ^{4}He. When we see that one temperature is sufficiently low for deuterons to last long enough to undergo proton and neutron captures, free neutrons are transformed into bound ones and the total number in the Universe stays more or less constant until start of stellar nucleosynthesis at much later stages in the evolution of our Universe.

As we know, nuclei of mass 8 are a *bottleneck* [126]. Two helium nuclei fuse to form ^{8}Be, but the next step, the fusion of ^{8}Be with a third helium nucleus is rare, since ^{8}Be is unstable with a half-life of $\simeq 10^{-16}$ s. Thus to form carbon, three helium nuclei must react [41]. This is not possible in the Big Bang because of rapid expansion [39, 40]. Thus because of the instability of ^{8}Be, all nuclei heavier than ^{7}Li must have been produced in stars. As will be shown below, carbon is formed from three helium nuclei (α-particles) in the interior of higher-mass stars, where high densities and temperatures are present for $\sim 10^6$ years. Von Weizsäcker [127] and Bethe [128] proposed a quantitative scheme by which the Sun produced energy. This process is the so-called *CNO* (carbon–nitrogen–oxygen) cycle (see, also [129, 130]). In this process, carbon acts as a catalyst; in equilibrium the net effect is the conversion of hydrogen into helium. Later a cycle involving the fusion of protons to produce helium, the *p–p* cycle [38] was found to be effective in lower-mass stars [39, 40]

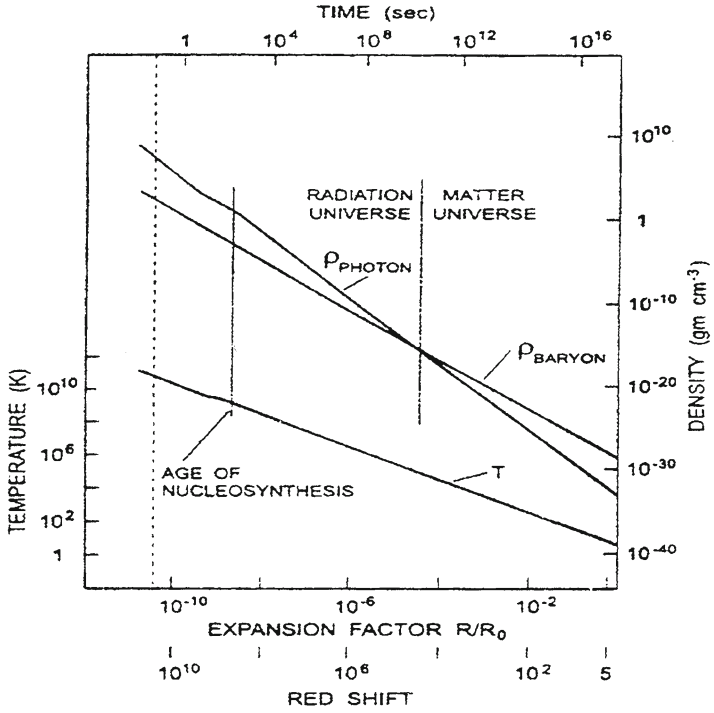

Fig. 2.18 A simplified presentation of the temperature and density relations in the homogenous Big Bang. The scale on the right vertical axis refers to the two upper curves for the photon and matter densities. The scale on the left vertical axis refers to the lowermost curve, which describes the temperature of the photon field. The remnant photon field of the Big Bang is a black body characterised by $T_{BG} = 2.75(1 + z)$. The production of the light elements occurred when the temperature fell below 2×10^9 K. This was the age of nucleosynthesis in the Big Bang. Following this time, the expansion allowed further cooling so that Big Bang nucleosynthesis came to an end. Matter continued to be ionized until the temperature fell below $\sim 10^3$ K. When the ions recombined matter became neutral and photons and matter decoupled. Following this was a period before stars and galaxies formed, the so-called 'dark age'. It is currently believed that star formation began at $z \sim 5$. The temperature contribution shown is the result of only the Big Bang contribution. Star formation will raise the temperature and perhaps re-ionize the Universe at $z \sim 5$ (after [129, 130]

In stars, the material becomes inhomogeneous since deeper in the interior the pressures and temperatures must be larger. In a similar way, the centres of stars more massive than the Sun must be hotter than the centre of the Sun; heavier elements are produced in higher-mass stars which have larger central temperature [39, 40, 125, 126]. To produce the nuclei of heavier elements by fusion, the larger *Coulomb's* repulsive forces must be overcome. These can only be produced in the centres of larger mass stars. Thus, only higher-mass stars can enrich the interstellar medium with nucleosynthesis products such as carbon, oxygen, neon or silicon. The exact yields of such

Table 2.10 Characteristics of the leptons

Flawor	Electric charge (e)	Spin	Mass (Gev/c^2)
ν_e—electron neutrino	0	1/2	$<7\times10^{-9}$
e^-—electron	−1	1/2	0.000511
ν_μ—muon neutrino	0	1/2	<0.00027
μ^-—muon (mu - minus)	−1	1/2	0.106
ν_τ—tau neutrino	0	1/2	<0.03
τ^-—tau (tau - minus)	−1	1/2	1.771

material are not certain since the product yields of such explosive processes depend on many details (for details, see [39, 40]).

When the hydrogen fuel is used up in a star, production of nuclear energy from fusing protons into ^{4}He stops and the temperature drops [129, 130]. Helium burning requires a temperature in the order of 10^8 K. Since ^{8}Be is unstable and lives only $\sim10^{-16}$ s, the conversation takes place mainly through the triple-α reaction

$$^4\text{He} +^4 \text{He} +^4 \text{He} \longrightarrow {}^{12}C + \gamma. \tag{2.35}$$

The ^{12}C produced can capture another α-particle to make ^{16}O,

$$^4\text{He} +^{12} \text{C} \longrightarrow {}^{16}\text{O} + \gamma. \tag{2.36}$$

In (2.35) and (2.36) γ is a electromagnetic radiation. Further α-particle capture produces even heavier nuclei. However, as we move to heavier and heavier nuclei, the *Coulomb's barrier* increases in height. This calls for higher temperatures that can come only from further gravitational contraction, as shown in Table 2.10. Since this is more likely to take place first at the centre, the inner parts of the star go to higher temperatures and densities, and evolve faster through different stages, than those outside.

The release of fusion energy stops at A $\approx$ 56, where the *binding energy* per nucleon peaks in value (see above). This takes place first in the stellar core and most of the nuclei are in the form of ^{56}Fe and ^{56}Ni the two most stable A = 56 *isobars*. Further evolution of the star depends even more critically on its total mass than any of its early stages. If the value is more than 8 times the solar mass [39, 40] there is enough gravitational energy left in the core in the core at the end of fusion to turn the star into a supernova.

When all the available ^{4}He in the central part of a star is used up, the core goes through another stage of gravitational contraction and rise in temperature. When $T \sim 10^9$ K, corresponding $kT \sim 100$ keV, reactions involving the conversion of any ^{12}C remaining after helium burning become possible, such as

$$
\begin{aligned}
{}^{12}\mathrm{C} + {}^{12}\mathrm{C} &\longrightarrow {}^{24}\mathrm{Mg} + \gamma \\
&\longrightarrow {}^{23}\mathrm{Na} + \mathrm{p} \\
&\longrightarrow {}^{23}\mathrm{Mg} + \mathrm{n} \\
&\longrightarrow {}^{20}\mathrm{Ne} + \alpha \\
&\longrightarrow {}^{16}\mathrm{O} + \alpha + \alpha. \qquad (2.37)
\end{aligned}
$$

The time span for the carbon *burning phase* is several orders of magnitude shorter than that for helium.

At even higher temperature, 2 to 3 $\times 10^9$ K, it is possible to convert ^{16}O into heavier elements, for example.

$$
\begin{aligned}
{}^{16}\mathrm{O} + {}^{16}\mathrm{O} &\longrightarrow {}^{32}\mathrm{S} + \gamma, \\
&\longrightarrow {}^{31}\mathrm{P} + \mathrm{p} \\
&\longrightarrow {}^{31}\mathrm{S} + \mathrm{n} \\
&\longrightarrow {}^{28}\mathrm{Si} + \alpha \\
&\longrightarrow {}^{24}\mathrm{Mg} + \alpha + \alpha. \qquad (2.38)
\end{aligned}
$$

When the temperature is between 3 and 4 $\times 10^9$ K, conversion of two ^{29}Si to one ^{56}Ni becomes possible.

Supernovas hold a special place in nucleosynthesis because of the heavy elements they produce. Since binding energy per nucleon decreases beyond A $\sim$ 56, it takes energy to create elements that are heavier (for details see [39, 129, 130]).

2.4 Isotope Effect in Nuclear Physics

In this section we will describe the influence of neutrons on the charge distribution. This influence has been studied using isotopic shift, the difference in the charge distributions of nuclei with the same number of protons but a different number of neutrons. If charge distribution in a nucleus is independent of neutrons, we expect the isotopic difference to be negligible. The measured results (see, e.g. [131–138]) indicate that, in general, the shifts are small but nonzero. Isotope shift (of spectral lines) can be divided into two classes that caused by the mass effect and that resulting from the field effect–volume effect. The mass effect consists of two parts, normal and specific, and results from the nucleus having a finite mass (see, also [41]). The *normal mass effect* can be calculated exactly, while the specific (for details see, also Chap. 4) mass effect present in spectra of atoms with more than one electron is very difficult to calculate precisely. Both of this effects decrease with increasing Z. The *field effect*, which increases with increasing Z, arises because of the deviation of the nuclear electric field from a Coulomb's field and can be used to study details of

Table 2.11 The root-mean-square radius ($\langle r^2 \rangle^{1/2}$) for detailed calcium isotopes

Nucleus	^{40}Ca	^{42}Ca	^{44}Ca	^{48}Ca
$\langle r^2 \rangle^{1/2}$ (fm)	3.4869	3.5166	3.5149	3.4762

nuclear structure. This is probably the most important consequence of isotope shift studies.

Thus in the very light elements the mass effect dominates and can account qualitatively for the observed shifts. In the heaviest elements the mass effect is negligible and the field effect can roughly account for the observed shift. In the element of intermediate mass the two effects are comparable. As a result, the shifts observed are small because the mass and field effects within the levels are often in such a direction as to oppose one another. In order to use the field effect in the demonstration of nuclear properties, it is necessary that the contribution of the mass and field effects to be observed shifts be known.

Isotope effect in calcium isotopes. The isotopic shift data [131], obtained from electron scattering, are summarized in Table 2.11. As we can see, the difference in the *root-mean-square radius* $\langle r^2 \rangle^{1/2}$ between the isotopes given in Table 2.11 are quite small. However, the good accuracies achieved in the measured values indicate a genuine difference among them. Since the radius decreases by 0.01 fm in going from ^{40}Ca to ^{48}Ca, it means that the addition of neutrons to calcium isotopes reduces the size of the charge distribution of the same 20 protons when neutron number is increased from 20 to 28. If we take the simple view that charges were distributed evenly throughout the nuclear volume, the charge radius should have increased by 6% based on simple $R = r_0 A^{1/3}$ relation. This is found to be true in the case of ^{48}Ti [131], a nucleus with two more protons and six more neutrons than ^{40}Ca. Here, the size of the charge distribution in increased by 0.1 fm for ^{48}Ti not far from the expectation of an $A^{1/3}$ dependence, instead of decreasing for ^{48}Ca. There are two possible explanations for the decrease in the charge radius with increasing neutron number among even calcium isotopes. The first is that addition of neutrons makes the protons more tightly bound and, hence, the charge radius is smaller. This is, however, not true for nuclei in general (see, e.g. [5, 9]). A second explanation is based on the charge distribution within a neutron (see, Fig. 2.3). One possible model for the charge distribution in a neutron is that the central part is positive and the region near the surface is negative, as shown in Fig. 2.3. The detailed charge distribution is not well known, because of the difficulty in measuring the small charge form-factor (see, also [132–134]). However, a small excess of negative charge in the surface region can produce about a third of decrease in the charge radius in going from ^{40}Ca to ^{48}Ca, as suggested by the authors of paper [142]. The other two-thirds may be attributed to the spin dependence in interactions of protons with other nucleons in the nucleus (see, e.g. [72, 73, 84, 85]). Regardless of the exact cause of the isotopic shift among calcium isotopes, it is clear that neutrons have a definite influence on the measured charge distribution of a nucleus (for details see [131–137]). The same effect can also

observed in other measurement, for example, such as the energy scattering of X-rays from muonic atoms [139–141].

Isotopic shift in muonic atoms. As was shown above, a muon is a lepton with properties very similar to an electron. For this reason, it is possible to replace one of the electrons on an atom by a (negative) muon to form muonic atom. However, since the mass of a muon is 209 times larger than that of an electron, the radii of the muonic orbits are much smaller than those of electrons.

According atomic physics (see, e.g. [139]) hydrogen-like atom with Z *protons* in the nucleus and only a single electron outside, the radius of the *n*th orbit is given by

$$r_n(e^-) = \frac{n^2\hbar^2}{\alpha\hbar c Z m_e} \tag{2.39}$$

Here, m_e is the mass of an electron, α is the fine structure constant. For hydrogen atom (Z = 1), the ground state (n = 1) radius is well known *Bohr radius* (see, also [139]);

$$a_0 = \frac{\hbar}{\alpha \mathrm{c} m_e} = 5.29\times10^{-11}\,\mathrm{m}. \tag{2.40}$$

Using (2.40), we can obtain the analogous results for a muonic atom by replacing m_e by m_μ

$$r_n(\mu^-) = a_0 \frac{n^2 m_e}{Z m_\mu}. \tag{2.41}$$

Using a muon mass $m_\mu = 106\,\mathrm{MeV/c^2}$, we obtain for a heavy nucleus, such as ^{208}Pb (Z = 82) the radius of the lowest muonic orbit

$$r_1(\mu^-) \simeq 3.1\times10^{-15}\,\mathrm{m} \tag{2.42}$$

or 3.1 fm. This is actually smaller than the value of 7.1 fm for the radius of ^{208}Pb, estimated using $\mathrm{R} = \mathrm{r_0 A^{1/3}}$ with $\mathrm{r_0} = 1.2$ fm [8]. A more elaborate calculation [140] shows that the muon spends inside a heavy nucleus. Being very close to the nuclear surface, the low-lying muonic orbits are sensitive to the detailed charge distribution of the different isotopes. The resulting changes in the energy levels may be observed as shifts in position of lines. Detailed investigation of isotopic shift was done on the different isotopes of Fe in paper by Shera et al. [140]. Muonic X-ray spectra from three isotopes of Fe obtained in this chapter are shown in Fig. 2.19. The isotope shift is large compared with isotope shift of electronic X-rays, which is typically 10^{-2} eV per unit change in A.

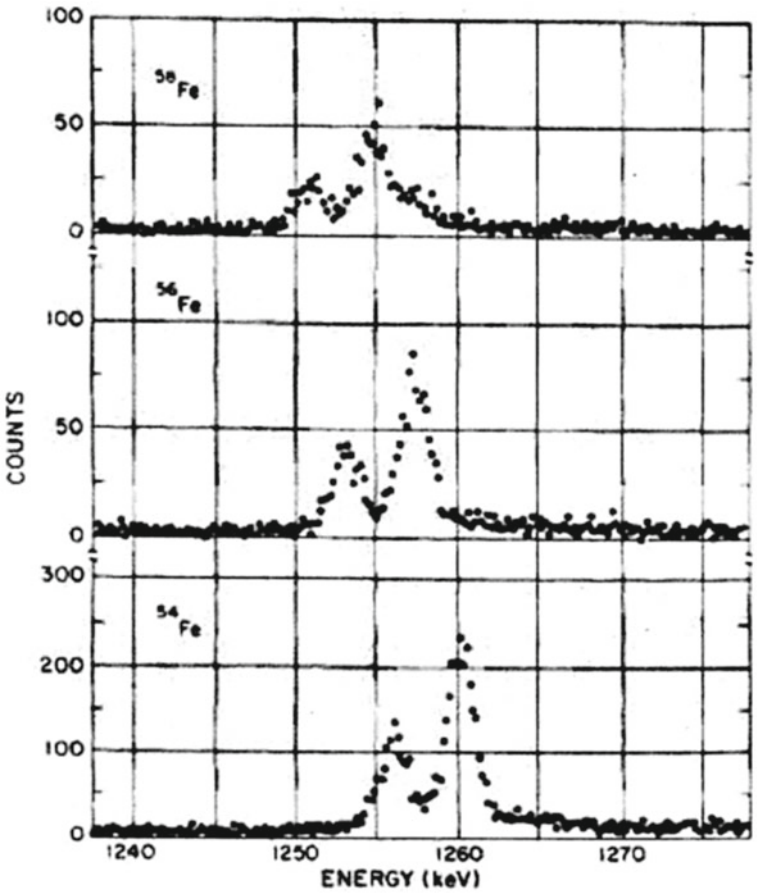

Fig. 2.19 Typical spectra showing the muonic $2p$–$1s$ X-ray doublet for three isotopes of Fe. The two peaks show the $2p_{3/2} \rightarrow 1s_{1/2}$ and $2p_{1/2} \rightarrow 1s_{1/2}$ transitions in the ratio 2:1 determined by the the statistical weight $(2j + 1)$ of the initial initial state. The isotope shift can clearly be seen as the change in energy of the transitions (after [140])

2.5 The Origin of the Mass

As we know well, that in a nucleus the protons and neutrons, collectively known as *nucleons*, are bound together by the strong nuclear force. At a fundamental level these interactions are described by Quantum Chromodynamics (*QCD*), a theory of quarks and gluons carrying colour charges that are asymptotically free at short distances. However, the quarks and gluons in a nucleus are very far from being asymptotically-free. Instead they comprise individual, colourless nucleons, which largely retain their identity in the many-body system. The colour-singlet nucleons are then bound to each other by what can be thought of as 'residual' QCD strong interactions. This sketch

of nuclear dynamics from the QCD point of view—brief as it is—makes it clear that from this standpoint the nucleus is an incredibly complicated, nonperturbative, quantum-field-theoretic, infinite-body problem.

Understanding the nucleon mass and its dependence of light *quark masses* is clearly one of the most fundamental issues [43, 47, 140] in nuclear and particle physics (see, also [143–152]). A key question concerns the origin of the nucleon mass: how do almost massless u and d quarks and massless gluons cooperate dynamically to form a localized baryonic compound with a mass of almost 1 GeV? An equally fundamental issue is the origin of the nucleon spin: how is the total angular momentum of the nucleon in its rest frame distributed between its quarks and gluons and in turn between their spin and orbital angular momentum? We will not discuss the last question here further (for details, see e.g. [152, 153]).

As we all know, almost all of the mass of the visible *Universe* is determined by the mass of the sum of the masses of nucleons in the cosmos. The *gluonic energy density* in the presence of three localized valence quarks obviously plays a decisive role in generating the nucleon mass [47, 149]. Basic *QCD* symmetries and the corresponding conserved currents as a guiding principle to construct effective Lagrangians which represent QCD at low energies and momenta. A rapidly advancing approach to deal with non-perturbative QCD is Lattice Gauge Field Theory (see, e.g. [154–160]). Considerable progress is being made solving QCD on a discretised Euclidean space–time lattice using powerful computers (for details, see [150, 151] and references therein). Lattice QCD has progressed to the joint that it can give reliable results concerning this issue, but with input quark masses still typically in order of magnitude larger than the actual current quark masses entering the QCD Lagrangian. Combining CHPT with lattice QCD has thus become a widely used routine in recent years (see, e.g. Fig. 2.1 in [150, 151]).

To better understand the origin of the mass we should analyse the *QCD condensates*. In QCD by condensates there are the vacuum mean values $< 0 \mid \mathbb{Q} \mid 0 >$ of the local (i.e. taken at a single point of space-time) operator $\mathbb{Q}_i(x)$ which are due to *non-perturbative effects*. When determining vacuum condensates one implies the averaging only over non-perturbative fluctuations. If for some operator $\mathbb{Q}_i$ the non-zero vacuum mean value appears also in the perturbation theory, it should not be taken into account in determination of the condensate. In other words when determining condensates the perturbative vacuum mean values should be substracted in calculation of the vacuum averages. As we know, the *perturbation theory* series in QCD is asymptotic series. So, vacuum mean operator values appear due to one or another summing of asymptotic series. The vacuum mean values of such kind are commonly to be referred as vacuum condensates [161]. The non-zero value of *quark condensate* means the transition of left-hand quark fields into right-hand ones and is not small value would mean to chiral symmetry violation in QCD. Quark condensate may be considered as an order parameter in QCD corresponding to spontaneous violation of the chiral symmetry [154–160].

For quark condensate $<0 \mid \overline{q}q \mid 0>$ ($q = u, d$ are the fields of u and d quarks) there holds the Gell-Mann-Oakes-Renner (GMOR) relation [162]

$$< 0 \mid \overline{q}\mathrm{q} \mid 0 >= -\frac{1}{2}\frac{m_\pi^2 f_\pi^2}{m_u + m_d}. \tag{2.43}$$

Here m_π, f_π are the mass and constant of π^+-meson decay ($m_\pi = 140\,\mathrm{MeV}$, $f_\pi =$ 92–131 MeV for different authors), m_u and m_d are the masses of u- and d-quarks. Relation (2.43) is obtained in the first order of m_u, m_d, m_s (for its derivation see, e.g. [45]). To estimate the value of quark condensate one may use the values of quark masses $m_u + m_d = 13$ MeV [163]. Substituting these values into (2.43) we get for quark condensate

$$< 0 \mid \overline{q}\mathrm{q} \mid 0 >= -(0.23\,\mathrm{GeV})^3 \simeq -1.6\,\mathrm{fm}^{-3}, \tag{2.44}$$

This condensate is a measure, as note above, of spontaneous chiral symmetry breaking. The non-zero pion mass, on the other hand, reflects the explicit symmetry breaking by the small quark masses, with $m_\pi^2 \sim m_q$. It is important to note that m_q and $< 0 \mid \overline{q}\mathrm{q} \mid 0 >$ are both scale-dependent quantities. Only their product $\mathrm{m}_q < 0 \mid \overline{q}\mathrm{q} \mid 0 >$ is scale independent, i.e. invariant under the renormalisation group.

The appearance of the mass gap $\Gamma \sim 1$ GeV in the *hadron* spectrum is thought to be closely linked to the presence of chiral condensate $< 0 \mid \overline{q}\mathrm{q} \mid 0 >$ in the QCD ground state. Ioffe formula [164], based on QCD sum rules, connects the nucleon mass M_N directly with quark condensate in leading order

$$\mathrm{M}_N = -\left[\frac{8\pi^2}{\Lambda_B^2} < 0 \mid \overline{q}q \mid 0 >\right]^{1/3} + \cdots \tag{2.45}$$

where $\Delta_B \sim 1\,\mathrm{GeV}$ is an auxiliary scale (the Borel mass [150, 151]) which separates "short" and "long" distance in the QCD sum rule analysis. While Ioffe's formula needs to be improved by including condensates of higher dimensions, it nevertheless demonstrates the close connection between dynamical mass generation and spontaneous chiral symmetry breaking n QCD. Taking into account the value of quark condensate from Eq. (2.44) we get for M_N

$$\mathrm{M}_N = 986.4\,\mathrm{MeV} \tag{2.46}$$

The obtained value of M_N differs from experimental meaning of $\mathrm{M}_N = 940$ MeV on the 5%. For nuclear physics, Eqs. (2.45–2.46) give important hint: the change of the quark condensate with increasing baryon density implies a significant reduction of the nucleon mass in the nuclear medium.

In the *chiral effective theory*, the *quark mass* dependence of M_N translates into dependence on the pion mass at leading order. The systematic chiral expansion [155–160] of the nucleon mass gives an expression of the form

$$\mathrm{M}_N = \mathrm{M}_0 + c\mathrm{m}_\pi^2 + d\mathrm{m}_\pi^4 - \frac{3\pi}{2} g_A^2 m_\pi \left(\frac{\mathrm{m}_\pi}{4\pi f_\pi}\right)^2 \left(1 - \frac{m_\pi^2}{8\mathrm{M}_0^2}\right) + \cdots \tag{2.47}$$

where the coefficients c and d multiplying even powers of the pion mass include low-energy constants constrained by *pion-nucleon scattering*. Note that the coefficient d also involves a $\log \mathrm{m}_\pi$ term.

In conclusion of this section we should note the fact m_d is larger than m_u by a few MeV implies that the neutron is heavier than the proton by a few MeV. As is well known, the experimental neutron–proton mass difference of $\mathrm{M}_n - \mathrm{M}_p = 1.2933317 \pm 0.0000005$ MeV [68, 94] receives an estimated electromagnetic contribution of [143] $\mathrm{M}_n - \mathrm{M}_p \mid^{em} = -0.76 \pm 0.30$ MeV and the remaining mass difference is due to a strong isospin breaking contribution $\mathrm{M}_n - \mathrm{M}_\mathrm{p} \mid^{d-\mathrm{u}} = 2.05 \pm 0.30$ MeV. Recently Bean et al. [152] have performed the first lattice calculation of the neutron–proton mass difference arising from the difference between the mass of the up and down quarks (see, also [165–168] and find $\mathrm{M}_n - \mathrm{M}_p \mid^{d-\mathrm{u}} = 2.26 \pm 0.57$ MeV). This value is in good agreement with the experimental result quoted. Concluding we should note, that we do not know why the observed mass pattern ($\mathrm{M}_n, \mathrm{M}_p, \mathrm{m}_u, \mathrm{m}_d$ etc.) looks like this, but nuclear physics can analyse the consequence of this empirical fact.

2.6 New Physics Beyond the Standard Model

A major challenge for physics today is to find the fundamental theory beyond the *Standard Model* [47] (the "Theory of everything"). In a nutshell, the standard model (SM) is a unified gauge theory of the strong, weak and electromagnetic interactions, the content which is summarised by the group theory

$$\mathrm{SU}(3)_C \times \mathrm{SU}(2)_L \times \mathrm{U}(1)_Y \tag{2.48}$$

where the first factor refers to the theory of strong interactions, or Quantum Chromodynamics (*QCD*) [149, 155–160], and the latter two factors describe the theory of electroweak interactions (see, also [42, 48–52, 99, 169]). However, we have the difficulty that the vast majority of the available experimental information, at least in principle [170–174], explained by the SM (see, also [175]. Also, until now, there has been no convincing evidence for existence of any particles other than those of the SM and states composed of SM particles. All accelerator physics seems to fit well with the SM, except for *neutrino* oscillations [42]. Apart from neutrino masses and mixing angles the only phenological evidence for going beyond the SM comes from cosmology and astrophysics [176–182]. It is well known that the pure SM predicts a too low value for the baryon number resulting from the Big Bang [1]. Apart from these astrophysical problems, there is only very weak experimental evidence for effects which do not match the SM extended to include neutrino mass as well

as hierarchy of elementary particles mass, etc. From these standpoints, the SM has been an enormously successful theory. Nevertheless, there exist many reasons for believing that the SM is not the end of the story. Perhaps the most obvious is the number of independent parameters that must be put in by hand. For example, the minimal version of the SM has 21 free parameters, assuming massless neutrinos and not accounting electric charge assignments [48–52]. Most physicists believe that this is just too much for the fundamental theory. The complications of the SM can also be described in terms of a number of problems, which we list briefly below.

1. Coupling Unification.
   There exists a strongly held belief among particle physicists and cosmologists that in the first moments of the life of the *Universe*, all forces of nature were "unified", that is they all fit into a single gauge group structure whose interaction strengths were described by a single coupling parameter, g_u (see, Fig. 2.2. in [43]). As we can see from this figure, that the three SM coupling almost meet at a common point around 3×10^{16} GeV.
2. The Hierarchy Problem.
   As we know, all matter under ordinary terrestial conditions can be constructed on the fermions (ν_e, e^-, u, d) of the first family (see Table 2.9). Yet we also know from laboratory studies that there are two families $(\nu_{\mu,}\mu^-, c, s)$ and (ν_τ, τ^-, t, b) that are heavier copies of the first family with no obvious role in nature. The SM gives no explanation for the existence of these heavies families. Futhermore, there is no explanation or prediction of the fermion masses, which over at least five orders of magnitude:

$$\mathrm{M}_{W,Z} \sim \mathrm{m}_{top} \gg \mathrm{m}_b \gg \mathrm{m}_\tau \gg \mathrm{m}_e \gg \mathrm{m}_\nu. \tag{2.49}$$

   How does one explain this hierarchy of masses? The SM gives us no clue as to how to explain the hierarchy problem. Really, the problem is just too complicated. Simple grand unified theory (*GUT*) does not help very much with this (for details see e.g. [48–52] and references therein). We should repeat that the non-vanishing neutrino masses and mixings are direct evidence for new physics beyond the SM.
3. Discrete Symmetry Violation.
   By construction, the SM is maximally parity-violating, it was built to account for observations that weak c.c. processes involve left-handed particles (or right-handed antiparticles). But why this mismatch between right-handness and left-handness? Again no deeper reason for the violation of parity is apparent from the SM. It would be desirable to have answer to this question, but it will take some new framework to provide them.
4. *Baryon* Asymmetry of the *Universe*.
   Why do we observe more matter than antimatter? This is problem for both cosmology and the SM.
5. Graviton Problem.
   Gravity is not fundamentally unified with other interactions in the SM, although it is possible to graft on classical general relativity by hand. However, this is not

a quantum theory, and there is no obvious way to generate one within the *SM* context. In addition to the fact that gravity is not unified and not quantised there is another difficulty, namely the cosmological constant (for details, see [176–182] and references therein). The cosmological constant can be thought of as energy of the vacuum. The energy density induced by spontaneous symmetry breaking is some $\sim$120 orders of magnitude larger than the observational upper limit. This implies the necessity of severe fine-tuning between the generated and bare pieces, which do not have any a priori reason to be related (see, also [183–185]).

6. Quantisation of Electric Charge.
   The SM does not motivate electromagnetic charge quantisation (for example, for quarks), but simply takes it as an input. The deeper origin of charge quantisation is not apparent from the SM (for the details, see also [185, 186]).

To summarize, despite the triumphant success of the SM, there exist conceptual motivations for believing that there is something more that the high energy desert is not so barren after all.

References

1. M. Gell-Mann, *The Quark and the Jaguar* (W.H. Freeman and Co., Adventures in the Simple and the Complex) (New York, 1997)
2. A.E.S. Green, *Nuclear physics* (McCraw-Hill, New York, 1955)
3. I. Kaplan, *Nuclear Physics*, 2nd ed. (Addison-Wesley, New York, 2002)
4. W.E. Burcham, 1973, Nuclear Physics. An Introduction. 2nd ed. (New York, Longman)
5. K.S. Krane, *Introductory Nuclear Physics* (Wiley and Sons, New York-Chichester, 1988)
6. J. Lilley, *Nuclear Physics* (Wiley and Sons, Chichester, 2001)
7. S.M. Wong, *Introductory Nuclear Physics* (Wiley and Sons, Chichester, 1998)
8. P.E. Hodgston, E. Gadioli, E. Gadioli-Erba, *Introductory Nuclear Physics* (Oxford University Press, Oxford-New York, 2000)
9. K. Heyde, *Basic Ideas and Concepts in Nuclear Physics* (Bristol-Philadelphia, IOP, 2004)
10. Ju.M. Schirokov and N.P. Judin, Nuclear Physics (Moscow, Science, 1980) (in Russian)
11. R.E. Taylor, Deep inelastic scattering: the early years. Rev. Mod. Phys. **63**, 573–585 (1991)
12. H.W. Kendall, Deep inelastic scattering: experiments on the proton and the observation of scattering, ibid, 63, 597–614 (1991).
13. J.I. Friedman, Deep inelastic scattering: comparison with quark model, ibid, 63, 615–627 (1991).
14. F.A. Wilczek, The cosmic assymmetry between matter and antimatter, Uspekhi Fiz. Nauk 175, 149–165 (2005) (in Russian).
15. F. Halzen, D. Martin, *Quarks and Leptons* (Wiley, New York, 1984)
16. A.P. Striganov and Ju.P. Donzov, Isotope effect in atomic spectra, Usp. Fiz. Nauk 55, 315–330 (1955) (in Russian).
17. S.E. Frish, Optical Spectra of Atoms (Moscow-Leningrad, Fizmatgiz, 1963) (in Russian)
18. I.I. Sobel'man, Itroduction in Theory of Atomic Spectra, 2nd edn (Moscow, Science, 1977) (in Russian)
19. W.H. King, *Isotope Shift in Atomic Spectra* (Plenum Press, New York, 1984)
20. M.A. Eliashevich, Atomic and Molecular Spectroscopy (Moscow, Fizmatgiz, 1962) (in Russian)
21. G. Herzberg, *Molecular Spectra and Molecular Structure* (D. van Nostrand, New York, 1951)

22. E.B. Wilson Jr, J.C. Decius, P.C. Gross, *Molecular Vibrations* (McGraw-Hill, The Theory of Infrared and Raman Vibrational Spectra (New York, 1955)
23. V.G. Plekhanov, Elementary excitation in isotope—mixed crystals. Phys. Reports **410**, 1–235 (2005)
24. M. Cardona, M.L.W. Thewalt, Isotope effect on optical spectra of semiconductors. Rev. Mod. Phys. **77**, 1173–1224 (2005)
25. V.G. Plekhanov, Fundamentals and applications of isotope effect in solids. Progr. Mat. Science **51**, 287–426 (2006)
26. V.G. Plekhanov, *Giant Isotope Effect in Solids* (Stefan University Press, La Jola, 2004). (USA)
27. V.G. Plekhanov, Applications of isotope effect in solids. J. Mater. Science **38**, 3341–3429 (2003)
28. G. Schatz, A. Weidinger, A. Gardener, *Nuclear Condensed Matter Physics*, 2nd edn. (Wiley, New York, 1996)
29. V.G. Plekhanov, *Applications of the Isotopic Effect in Solids* (Springer, Berlin, 2004)
30. D. Forkel - Wirth, Exploring solid state physics properties with radioactive isotopes, Rep. Progr. Phys. 62, 527–597 (1999).
31. M. Deicher, *Radioactive ion beams: applications to semiconductor physics* (Analysis in Materials Science, Freiberg, June, 2005), pp. 15–17
32. S.I. Adelstein, F.Y. Manning (eds.), *Isotopes for Medicine and Life Science* (National Academy Press, Washington, 1995)
33. L.L. Gol'din, M.F. Lomanov, V.B. Savchenko et al., Uspekhi-Phys (Moscow) 110, 77–100 (1973) (in Russian).
34. U. Amaldi, G. Kraft, Radiotherapy with beams of carbon ions. Rep. Progr. Phys. **68**, 1861–1883 (2005)
35. M.M. Ter-Pogossian, in Positron Emission Tomography, ed. by I. Reivich, A. Alovi (New York, Alan R. Press, 1985)
36. V.Ju. Baranov, (Ed.) Isotopes, Vol. 1 and 2 (Moscow, Fizmatlit, 2005) (in Russian)
37. O. Manuel, *Origins of Elements in the Solar Systems* (Kluwer Academic Press, New York, 2001)
38. E.M. Burbidge, G.R. Burbidge, W.A. Fowler, F. Hoyle, Synthesis of the elements in stars. Rev. Mod. Phys. **29**, 547–652 (1957)
39. G. Wallerstein, I. Jhen, Jr, P. Parker et al., Synthesis of the elements in stars: forty years in progress, ibid, 69, 995–1084 (1997).
40. S. Esposito, Primordial Nucleosynthesis: Accurate Prediction for Light Element Abundances, ArXiv:astro-ph/ 990441
41. V.G. Plekhanov, Manifestation and Origin of the Isotope Effect, ArXiv: gen. phys/0907.2024
42. E.H. Simmons, Top Physics, ArXiv, hep-ph/0011244
43. V.G. Plekhanov, *Isotope Low-Dimensional Structures* (Springer, Heidelberg-Berlin, 2012)
44. B.L. Ioffe, The origin of mass, Usp. Fiz. Nauk (Moscow) **176**, 1103–1104 (2006) (in Russian)
45. A.D. Dolgov and Ja.B. Zel'dovich, Cosmology and elementary particles, Rev. Mod. Phys. **53**, 1–41 (1981)
46. A.D. Linde, The inflated Universe, Usp. Fiz. Nauk **144**, 177–214 (1984) (in Russian)
47. B.L. Ioffe, Chiral effecrive theory of strong interactions, Usp. Fiz. Nauk **171**, 1273–1290 (2001) (in Russian)
48. P. Langacker, Structure of the Standard Model, ArXiv: hep-ph. 0304186
49. S. F. Novaes, Standart Model: An Introduction, ArXiv: hep-ph/00012839
50. C.D. Froggatt, H.B. Nielsen, Trying to Understand the Standard Model Parameters, ArXiv: hep-ph/0308144
51. J.F. Donoghue, E. Golowich, B.R. Holstein, *Dynamics of Standard Model* (Cambridge University Press, Cambridge, 1992)
52. C. Burgess, G. Moore, *Standard Model—A Primer* (Cambridge University Press, Cambridge, 2006)
53. I.I. Royzen, E.L. Feinberg, E.L. Chernavskaya, Color deconfinment and subhadronic matter: phase states and the role of constituent quarks, Usp. Fiz. Nauk **174**, 473–503 (2004) (in Russian)

54. W. Marciano, H. Pagels, Quantum chromodynamics. Phys. Reports **36**, 137–276 (1978)
55. D.W. Lee, *Chiral Dynamics* (Gordon and Breach, New York, 1972)
56. S. Coleman, *Aspects of Symmetry* (Cambridge University Press, Cambridge, 1985)
57. http://www.lbl.gov./abc/wallchart
58. F. Soddy, Intra—atomic charge. Nature (London) **92**, 399–400 (1913)
59. F. Soddy, The structure of the atom, Nature (London) **92**, 452–452 (1913)
60. H. Frauenfelder, E.M. Henley, *Subatomic Physics* (Prentice Hall, New York, 1991)
61. J.J. Kelly, Nucleon charge and magnerization densities from Sachs form factors. Phys. Rev. **C66**, 065203–065206 (2002)
62. G.A. Miller, A.K. Opper, E.J. Stephenson, Charge symmetry breaking and QCD, ArXiv: nucl.- ex/0602021
63. G.A. Miller, Charge densities of the neutron and proton. Phys. Rev. Lett. **99**, 112001–112004 (2007)
64. G.A. Miller, J. Arringfton, The neutron negative central charge density: an inclusive–exclusive connection, ArXiv: nucl-th/0903.1617.
65. C.M. Lederer, V.S. Shirley, *Table of Isotopes* (Wiley, New York, 1978)
66. F.W. Aston, Isotopes and atomic weights. Nature **105**, 617–619 (1921)
67. F.W. Aston, *Mass-Spectra and Isotopes*, (Science, Moscow, 1948) (in Russian)
68. R.N. Cahn, G.G. Goldhater, *The Experimental Foundations of Particle Physics* (Camdridge University Press, Camdridge, 1989)
69. R. Shurtleft, E. Derringh, Am. J. Phys. **47**, 552 (1989), cited in [68]
70. R.C. Barrett, D.F. Jackson, *Nuclear Sizes and Structure* (Clarendon Press, Oxford, 1977)
71. M. Waraquier, J. Morean, K. Heyde et al., Rearrangement effects in shell-model calculations using density—dependent interactions. Phys. Reports **148**, 249–291 (1987)
72. W.F. Hornyack, *Nuclear Structurs* (Academic, New York, 1975)
73. B.M. Brink, *Nuclear Forces* (Pergamon, New York, 1965)
74. J. Carlson, R. Schiavilla, Structure and dynamics of few—nucleon systems. Rev. Mod. Phys. **70**, 743–841 (1998)
75. C. Davies, S. Collins, *Physics* (World, August, 2000), pp. 35–40
76. L.I. Schiff, Scattering of neutrons by deuterons. Phys. Rev. **52**, 149–154 (1937)
77. S.S. Share, J.R. Stehn, Effect of long range forces on neutron–proton scattering. Phys. Rev. **52**, 48–52 (1937)
78. J. Schwinger, E. Teller, The scattering of neutrons by ortho–parahydrogen, Phys. Rev. **52**, 286–295 (1937)
79. G.L. Greene, E.G. Kessler, New determination binding energy and the neutron mass. Phys. Rev. Lett. **56**, 819–822 (1986)
80. S. Gartenhaus, Two-nucleon potential from the cut-off Yukawa theory. Phys. Rev. **100**, 900–905 (1955)
81. J.D. Walecka, *Theoretical Nuclear and Subnuclear Physics* (Oxford University Press Inc, New York, 1995)
82. D.J. Griffiths, *Introduction to Elementary Partcles* (Wiley, New York, 1987)
83. R.K. Adair, Neutron cross-sections of the elements. Rev. Mod. Phys. **22**, 249–298 (1950)
84. R. Wilson, *The Nucleon–Nucleon Interaction* (Wiley, New York, 1963)
85. E.M. Henley, J.P. Schiffer, Nuclear Physics, ArXiv: nucl-th / 9807041
86. E. Segre, *Nuclei and Particles* (Reading MA, Benjamin, New York, 1982)
87. R.A. Arndt, L.D. Roper, Nucleon–nucleon partiale-wave analysis to 1100 MeV. Phys. Rev. **D35**, 128–144 (1987)
88. R. Vinh Mau, in *Mesons in Nuclei*, ed. by M. Rho, D.H. Wilkinson, (North-Holland, Amsterdam, 1979)
89. R. Machleidt, K. Holinde, Ch. Elster, Phys. Rev. **149**, 1 (1987), cited in [88]
90. W. Heisenberg, Über den anschaulichen Inhalt der quantentheoretischen Kinematik und Mechanik. Zs. Physik **77**, 172–198 (1932)
91. P. Renton, *Electroweak Interactions: An Introduction to the Physics of Quarks and Leptons* (Cambridge University Press, Cambridge, 1990)

92. B.R. Holstein, *Weak Interactions in Nuclei* (Princeton University Press, Princeton, 1989)
93. E.A. Paschoes, *Electroweak Theory* (Cambridge University Press, Cambridge, 2007)
94. S. Edelman, Particle physics summary. Phys. Lett. B **592**, 1–101 (2004)
95. D.P. Roy, Basic constituents of matter and their interactions—A progress report: ArXiv: hep-ph/9912523
96. F. Wilczek, The Universe is a strange place, ArXiv: astro - ph/0401347
97. I.J.R. Aitchison, A.J.G. Hey, *Gauge Theories in Particle Physics: A Practical Introduction* (Adam Hilger, Bristol, 1990)
98. A. Volcarce, A. Fernandez, P. Gonzalez, Quark—model study of few—baryon systems. Rep. Progr. Phys. **68**, 965–1041 (2005)
99. W. Wagner, The quarks physics in hadron collisions, Rep. Progr. Phys. **68**, 2409–2494 (2005)
100. D.J. Gross, The discovery of asymptotic freedom and the emergance of QCD. Rev. Mod. Phys. **77**, 837–851 (2005)
101. D. Politzer, The dilemma of attribution, ibid, **77**, 851–857 (2005)
102. F. Wilczek, Asymptotic freedom: from paradox to paradigm, ibid, **77**, 857–871 (2005)
103. S.L. Glashow, Partial-symmetries of weak interactions. Nucl. Phys. **22**, 579–588 (1995)
104. S. Weinberg, A model of leptons. Phys. Rev. Lett. **19**, 1264–1267 (1967)
105. A. Salam, Elementary Particle Theory, in *Proceedings of the Eigth Nobel Symposium*, p. 367, 1968, ed. by N. Svartholm
106. S. Weinberg, The Making of the Standard Model, ArXiv: hep-ph /0401010
107. A. Abbas, Quarks and neutrons halo nuclei, nuclear clusters and nuclear molecules. Mod. Phys. Lett. **A16**, 755–761 (2001)
108. A. Abbas, Structure of A=6 nuclei ^{6}He, ^{6}Li and ^{6}Be, Mod. Phys. Lett. **A19**, 2365–2370 (2004)
109. F.I. Yndurain, *The Theory of Quark and Gluon Interactions* (Springer, Berlin, 1999)
110. H. Satz, The transition from hadron matter to quark-gluon plasma. Ann. Rev. Nucl. Sci. **35**, 245 (1985)
111. T. Celik, J. Engles, H. Satz, Finite temperature lattice QCD with Wilson fermions. Nucl. Phys. **B256**, 670–686 (1985)
112. S. Weinberg, *The First Three Minutes* (Basic Books, New York, 1993)
113. H.E. Suess, H.C. Urey, Abundances of the elements. Rev. Mod. Phys. **28**, 53–74 (1956)
114. G. Gamow, *One, Two, Three Infinity* (Viking Press, New York, 1947)
115. G. Gamow, Expanding Universe and the origin of elements, Phys. Rev. **70**, 572–573 (1946)
116. G. Gamow, The origin of elements and the separation Galaxes, Phys. Rev. **74**, 505–506 (1948)
117. R.A. Alpher, H.A. Bethe, G. Gamow, The origin of chemical elements. Phys. Rev. **73**, 803–804 (1948)
118. R.A. Alpher, R.C. Herman, Theory of the origin of relative abundance. Rev. Mod. Phys. **22**, 153–212 (1950)
119. Refelections on early work on "big-bang" cosmology, Phys. Today **41**, (No 8) 24–33 (1988)
120. C. Hayashi, Prog. Theor. Phys. 5, 224 (1950), cited in [101]
121. A.A. Penzias, R.W. Wilson, A measurements of excess antenna temperature at 4080 ms/c. Astrophys. J. **142**, 419–421 (1965)
122. A.A. Penzias, The Origin of the Elements, Nobel Lecture, December 8, 1978
123. J.C. Mather, Measurement of the cosmic microwave background spectrum by the COBE FIRAS instrument. Astrophys. J. **420**, 439–444 (1994)
124. F. Hoyle, R. Taylor, The mystery of the cosmic abundance. Nature **203**, 1108–1109 (1964)
125. D.N. Schramm, *Primordial Nuclei and Their Galactic Evolution*, ed. by N. Prantzos, M. Tosi, R. von Steiger (Kluwer, Dodrecht, 1998) p. 3
126. M. Arnould, K. Takahashi, Nuclear astrophysics. Rep. Prog. Phys. **62**, 395–464 (1999)
127. C.F. von Weizsacker, Zs. phys. **39**, 633 (1938) cited in [114–116]
128. H.A. Bethe, Energy production in stars. Phys. Rev. **55**, 434–456 (1939)
129. T.L. Wilson, Isotopes in the interstellar medium and circumstellar envelopes. Rep. Prog. Phys. **62**, 143–185 (1999)

130. K. Langanke and M. Wiescher, Nuclear reaction and stellar processes, ibid 64, 1657–1691 (2001)
131. R.F. Frosch, R. Hofstadter, J.R. McCarthy et al., Electron scattering studies of calcium and titanium isotopes. Phys. Rev. **174**, 1380–1389 (1968)
132. K. Heilig, A. Steudel, Changes in mean square nuclear charge radii from optical isotope shift. At. Data Nucl. Data Tables **14**, 613 (1974)
133. H.W. Brandt, K. Heilig, A. Steudel, Optical isotope shift measurements of ^{40,42,43,44,48}Ca by use of enriched isotopes in atomic beam. Phys. Lett. **A64**, 29–30 (1977)
134. F. Aufmuth, K. Heilig, A. Steudel, Changes in mean square nuclear charge radii from optical isotope shift. At. Data Nucl. Data Tables **37**, 455–490 (1987)
135. K. Blaum, High accuracy mass spectrometry with stored ions. Phys. Reports **425**, 1–783 (2006)
136. K. Blaum, W. Geithnar, J. Lassen. Nuclear moments and charge radii of argon isotopes between the neutron—shell closures N=20 and N=28, Nucl. Physics **799**, 30–45 (2008)
137. M. Glaser, M. Borys, Precision mass measurements. Rep. Prog. Phys. **72**, 126101–126131 (2009)
138. A. Kelic, K.-H. Schmidt, T. Enqvist, Isotopic and velocity distributions of ^{83}Bi produced in charge - pickup reactions of ^{82}Pb $_{208}$ at 1 GeV. Phys. Rev. **C70**, 064608–064612 (2004)
139. E.V. Shpol'sky, *Atomic Physics*, Part One. (Fiz-Mat Lit, Moscow, 1974) (in Russian)
140. E.B. Shera, E.T. Ritter, R.B. Perkins, Systematics of nuclear charge distributions in Fe, Co, Ni, Cu, and Zn fom muonic x-ray measurements. Phys. Rev. **C14**, 731–747 (1976)
141. P.L. Lee, F. Boehm, A.A. Hahn, Variations of nuclear charge radii in mercury isotopes with A = 198, 199, 200, 201, 202, and 204 from X-ray isotope shifts. Phys. Rev. **C17**, 1859–1861 (1978)
142. W. Bertolozii, J. Friar, J. Heisenberg, Contributions of neutrons to elastic electron scattering from nuclei. Phys. Lett. **B41**, 408–414 (1972)
143. The prehistory of quark masses is reviewed in J. Grasser, H. Leutwyller, Quark masses, Phys. Rep. **87**, 77–169 (1982)
144. H. Leutwyller, Masses of the light quarks, ArXiv: hep-ph/9405330
145. H. Leutwyller, ArXiv: hep-ph/ 9602255
146. H. Leutwyller, Insights and puzzles in light quark physics, ArXiv:hep-ph/ 07063138
147. C.D. Froggatt, The origin of mass. Surveys High Energy Phys. **18**, 77–99 (2003)
148. C.D. Froggatt, The Problem of mass, ArXiv: hep-ph/0312220
149. S. Narison, *in, QCD as a Theory of Hadrons: from Partons to Confinment* (Cambridge University Press, Cambridge, 2002)
150. M. Procura, B.U. Nusch, W. Weise, Nucleon mass: from lattice QCD to the chiral limit. Phys. Rev. **D73**, 114510–16 (2006)
151. B. Musch, Hadron masses, ArXiv: hep-ph/0602029
152. S.R. Beane, K. Orginos, M.J. Savage, Strong—isospin violation in the neutron–proton mass difference from fully—dynamical lattice QCD and PQQCD. Nucl. Phys. **B768**, 38–50 (2007)
153. B.L. Ioffe, Nucleon Spin Structure: Sum Rules, Arxiv:hep-ph/9511401
154. S. Scherer, M.R. Schindler, Chiral Perturbation Theory Primer, ArXiv:hep-ph/0505265
155. G. Ecker, Chiral Perturbation Theory, ArXiv:hep-ph/9501357
156. A. Pich, Chiral Perturbation Theory, ArXiv:hep-ph/9502366
157. S.R. Bean, P.F. Bedaque, W.C. Haxton., in "*At the Frontier of Particle Handbook of QCD*", ed. by M. Shifman (World Scientific, Singapoure, 2001), pp. 1–140
158. W. Weise, Yukawa's Pion, Low-Energy QCD and Nuclear Chiral Dynamics, ArXiv: nucl-th/ 0704.1992
159. J. Bijens, Chiral Perturbation Theory Beyon One Loop, ArXiv: hep-ph/0604043
160. J. Bijens, Progr. Part. Nucl. Phys. **58**, 521 (2007)
161. B.L. Ioffe, QCD at low energies. Progr. Part. Nucl. Phys. **56**, 232–277 (2006)
162. M. Gell-Mann, R.J. Oakes, B. Renner, Behavior of current divergences under SU_3 X SU_3 Phys. Rev. **175**, 2195–2199 (1968)

163. A. Pich, J. Prades, Tau - decay determination of the strange quark mass. Nucl. Phys. Proc. Suppl. **86**, 236–241 (2000)
164. B.L. Ioffe, Calculation of baryon masses in quantum chromodynamics. Nucl. Phys. **B188**, 317–341 (1981)
165. E. Epelbaum, U.-G. Meissner, W. Glöckle, Nucl. Phys. **A714**, 535 (2003)
166. U.-G. Meissner, Quark mass dependence of baryon properties, ArXiv: hep-ph/0509029
167. Müller B., 2007, From Quark-Gluon plasma to the perfect liquid, ArXiv: nucl-th/ 0710.3366
168. W. Weise, Overview and perspectives in nuclear physics, ArXiv: nucl-th/ 0801.1619
169. G. Altarelli, States of the Standard model and beyond. Nucl. Instr. and Methods **A518**, 1–8 (2004)
170. M. Pospelov, A. Ritz, Electric dipole moment as probes of new physics, ArXiv: hep-ph/0504231
171. M. Pospelov, A. Ritz, Annal. Phys. (NY) **318**, 119 (2005 (cited in [170]))
172. I.B. Khriplovich, S.K. Lamoreaux, *CP Violation Without Strangeness: Electric Dipole Moments of Particles, Atoms and Molecules* (Springer, Berlin, 1997)
173. A. Djouadi, The dichotomy of electroweak symmetry breaking: The Higgs boson and Standard model, Phys. Rep. **457**, 1–216 (2008)
174. M.J. Ramsey-Musolf, S. Su, Low-energy precision tests of supersymmetry, Phys. Rep., **456**, 1–137 (2008)
175. V.G. Plekhanov, The Enigma of the mass, ArXiv:gen. phys/0906.4408
176. C.S. Weinberg, The cosmological constant problem. Rev. Mod. Phys. **61**, 1–23 (1989)
177. C.S. Weinberg, The Cosmological constant problems, ArXiv:astro-ph/0005265
178. M. Tegmark, M.J. Rees, F. Wilczek, Dimensionless constants cosmology and other dark matters, ArXiv:astro-ph/0511774
179. A.D. Dolgov, Cosmology and new physics, ArXiv:hep-ph/0606230
180. T. Padmanabhan, Cosmological constant the weight of the vacuum. Phys. Rep. **380**, 235–320 (2003)
181. T. Padmanabhan, Dark energy: mystery of the millenium, ArXiv:astro-ph/0603114
182. G. Fuller, A. Hime, M. Ramsey-Musolf, Dark matter in, nuclear physics, ArXiv:nucl-ex/0702031
183. K.A. Milton, The Casimir effect: recent controversis and progress. J. Phys. A: Math. Gen. **37**, R209–R277 (2004)
184. S.K. Lamoreaux, The Casimir force: background, experiments and applications. Rep. Prog. Phys. **68**, 201–236 (2005)
185. S.K. Lamoreaux, The Casimir Force: Background, Experiments and Applications. Rep. Prog. Phys. **68**, 201–236 (2005)
186. M. Levin, X.-G. Wen, Photons and electrons as emergent phenomena. Rev. Mod. Phys. **77**, 871–897 (2005)

http://www.springer.com/978-3-642-28722-0

Isotopes in Condensed Matter
G. Plekhanov, V.
2013, XIV, 290 p., Hardcover
ISBN: 978-3-642-28722-0